

NAVAL POSTGRADUATE SCHOOL

Monterey, California



THESIS

J4748

AN EVALUATION OF COPLANAR LINE FOR
APPLICATION IN MICROWAVE
INTEGRATED CIRCUITRY

by

Jae Soon Jeong

December 1988

Thesis Advisor:

H.A. Atwater

Approved for public release; distribution is unlimited

1241982

REPORT DOCUMENTATION PAGE				
1a Report Security Classification Unclassified			1b Restrictive Markings	
2a Security Classification Authority			3 Distribution Availability of Report	
2b Declassification Downgrading Schedule			Approved for public release; distribution is unlimited.	
4 Performing Organization Report Number(s)			5 Monitoring Organization Report Number(s)	
6a Name of Performing Organization Naval Postgraduate School		6b Office Symbol (if applicable) 62	7a Name of Monitoring Organization Naval Postgraduate School	
6c Address (city, state, and ZIP code) Monterey, CA 93943-5000			7b Address (city, state, and ZIP code) Monterey, CA 93943-5000	
8a Name of Funding Sponsoring Organization		8b Office Symbol (if applicable)	9 Procurement Instrument Identification Number	
8c Address (city, state, and ZIP code)			10 Source of Funding Numbers	
			Program Element No	Project No
			Task No	Work Unit Accession No
11 Title (include security classification) AN EVALUATION OF COPLANAR LINE FOR APPLICATION IN MICROWAVE INTEGRATED CIRCUITRY				
12 Personal Author(s) Jae Soon Jeong				
13a Type of Report Master's Thesis		13b Time Covered From To		14 Date of Report (year, month, day) December 1988
15 Page Count 67				
16 Supplementary Notation The views expressed in this thesis are those of the author and do not reflect the official policy or position of the Department of Defense or the U.S. Government.				
17 Cosati Codes			18 Subject Terms (continue on reverse if necessary and identify by block number)	
Field	Group	Subgroup	Calculation for Impedance and Effective Dielectric Constant of Conductor-backed Coplanar Waveguide	
19 Abstract (continue on reverse if necessary and identify by block number) A general study of conductor backed coplanar waveguide is presented. The impedance (Z_0) and effective dielectric constant (ϵ_{eff}) of conductor-backed coplanar waveguide (CBCPW) have been calculated by using a variational method and the boundary point matching method. In this present work only the TEM dominant low frequency propagation mode of coplanar line has been considered. Experimental facilities are vector network analyzer (HP8409) and bench-instrument measurements.				
20 Distribution Availability of Abstract <input checked="" type="checkbox"/> unclassified unlimited <input type="checkbox"/> same as report <input type="checkbox"/> DTIC users			21 Abstract Security Classification Unclassified	
22a Name of Responsible Individual H.A. Atwater			22b Telephone (include Area code) (408) 646-3001	22c Office Symbol 62An

Approved for public release; distribution is unlimited.

An Evaluation of Coplanar Line for
Application in Microwave Integrated
Circuitry

by

Jae Soon Jeong
Captain, Korean Air Force
B.S., Korean Air Force Academy, 1981 Seoul

Submitted in partial fulfillment of the
requirements for the degree of

MASTER OF SCIENCE IN ELECTRICAL ENGINEERING

from the

NAVAL POSTGRADUATE SCHOOL
December 1988

ABSTRACT

A general study of conductor backed coplanar waveguide is presented. The impedance (Z_0) and effective dielectric constant (ϵ_{eff}) of conductor-backed coplanar waveguide (CBCPW) have been calculated by using a variational method and the boundary point matching method. In this present work only the TEM dominant low frequency propagation mode of coplanar line has been considered. Experimental facilities are vector network analyzer (HP8409) and bench-instrument measurements.

TABLE OF CONTENTS

I. INTRODUCTION	1
A. BACKGROUND	1
B. COPLANAR LINE TERMINOLOGY	1
II. ANALYSIS OF TEM PROPAGATION MODE	4
A. REVIEW OF ROWE & LAO BOUNDARY POINT MATCHING METHOD	4
B. REVIEW OF YAMASHITA'S VARIATIONAL METHOD	11
C. COMPARISON OF RESULTS	18
III. CONSTRUCTION OF COPLANAR LINES AND TRANSITIONS	28
A. ADHESIVE FOIL METHOD	28
B. PHOTOLITHOGRAPHICAL METHOD	30
C. TRANSITION TO COAXIAL LINE	30
IV. MEASUREMENT OF COPLANAR LINE PARAMETERS	33
A. RESONATOR METHOD FOR PHASE VELOCITY AND EFFECTIVE DIELECTRIC CONSTANT	33
1. Series Open-ended Resonator	33
2. Shunt Resonator	36
a. One-port Open-ended Resonator	36
b. Shunt Short-circuited Resonator	37
B. LEAKAGE WAVE MEASUREMENTS ON COPLANAR LINE AND MICROSTRIP	40
1. Measurement	40
2. Results	42
V. SUMMARY AND CONCLUSION	44

APPENDIX A. FORTRAN PROGRAM TO CALCULATE THE IMPEDANCE AND EFFECTIVE DIELECTRIC CONSTANT OF CBCPW USING BOUND- ARY POINT MATCHING METHOD	48
APPENDIX B. FORTRAN PROGRAM TO CALCULATE THE IMPEDANCE AND EFFECTIVE DIELECTRIC CONSTANT OF CBCPW USING VARI- ATIONAL METHOD	53
LIST OF REFERENCES	55
INITIAL DISTRIBUTION LIST	56

LIST OF TABLES

Table	1. COMPARISON OF THE EFFECTIVE DIELECTRIC CONSTANT . .	40
-------	--	----

LIST OF FIGURES

Figure 1. Coplanar systems	2
Figure 2. Conductor backed planar waveguides	2
Figure 3. Current flow characteristics of propagation modes	3
Figure 4. Geometry of a conductor backed CPW	5
Figure 5. Gaussian surface in the capacitance calculation	8
Figure 6. Calculated characteristic impedance of CBCPW by boundary point matching method	9
Figure 7. Calculated effective dielectric constant of CBCPW by boundary point matching method	10
Figure 8. Geometry of CBCPW	11
Figure 9. Assumed step-charge density function of CBCPW	13
Figure 10. Assumed linear-charge density function of CBCPW	14
Figure 11. Calculated characteristic impedance of CBCPW by variational method .	16
Figure 12. Calculated effective dielectric constant of CBCPW by variational method	17
Figure 13. Computed results for characteristic impedance versus strip width with line dimensions as parameters	20
Figure 14. Computed results for characteristic impedance versus strip width with line dimensions as parameters	21
Figure 15. Computed results for characteristic impedance versus strip width with line dimensions as parameters	22
Figure 16. Computed results for characteristic impedance versus strip width with line dimensions as parameters	23
Figure 17. Computed results for dielectric constant versus strip width for various line parameters	24
Figure 18. Computed results for dielectric constant versus strip width for various line parameters	25
Figure 19. Computed results for dielectric constant versus strip width for various line parameters	26
Figure 20. Computed results for dielectric constant versus strip width for various line parameters	27
Figure 21. Quarter wave length stub for substrate dielectric constant measurement	28

Figure 22. DB Magnitude plot for S_{21}	29
Figure 23. Drawn line pattern and negative	31
Figure 24. Series open-ended resonator and equivalent circuit	34
Figure 25. Plot for dB magnitude S_{21} versus frequency	35
Figure 26. Equivalent circuit for calculation of angle of impedance	36
Figure 27. Shunt shorted resonator and equivalent circuit	38
Figure 28. Plot for dB magnitude S_{21} with shunt shorted stub, and computed angle of impedance of $\frac{\lambda}{4}$ open stub at resonance	39
Figure 29. Line angle for conductor ambient field measurement	41
Figure 30. Block diagram for conductor ambient field measurement	41
Figure 31. Conductor ambient field distribution	43
Figure 32. Characteristic impedance versus strip width with dielectric constant as a parameter	46
Figure 33. Effective dielectric constant versus strip width with substrate dielectric constant as a parameter	47

ACKNOWLEDGEMENTS

I would like to thank the Korean Air Force for the opportunity to study at the Naval Postgraduate School.

I wish to thank Dr. H. A. Atwater for his patient guidance, continuous assistance and very helpful criticism through this work.

I am very grateful to Dr. R. Janaswamy whose comments and recommendations contributed to the successful completion of this thesis.

Finally, I am also grateful to my wife, Hye Yong, for her patience and thesis typing.

I. INTRODUCTION

A. BACKGROUND

In current microwave integrated circuit design practice, microstrip transmission line is almost universally employed for circuit construction. Although convenient and easily fabricated, microstrip line has the disadvantage of relatively high ambient field and coupling to outside circuits. Further, the incorporation of semiconductor devices and lumped elements into microstrip circuitry is difficult in that a *via* hole through the substrate must be introduced, in order to effect line to ground connection of the device.

Coplanar transmission line has the advantage that both line and ground conductors are available on the upper surface of the circuit, and devices are easily incorporated. In addition, the spurious coupling between coplanar lines and adjacent circuitry is known to be significantly lower than with microstrip. It is known, however, that spurious propagation modes and anomalous losses may occur on coplanar lines as a result of improper mode-excitation of the line, often due to incorrect termination of the coplanar ground planes [Ref. 1 , 2 , 3].

B. COPLANAR LINE TERMINOLOGY

The term coplanar line is generally applied to planar transmission systems in which a ground conductor accompanies the line that is *active* relative to ground return, on the surface of the dielectric substrate. In its original definition by Wen [Ref. 4], the term coplanar line referred to a system composed of a planar transmission line accompanied on two sides by ground planes (Figure 1a). The dielectric substrate was assumed to have effectively infinite thickness. The term *coplanar strips* is sometimes applied to a two-conductor system of line with single ground return (Figure 1b).

The widespread use of microstrip line for microwave integrated circuit construction, with a ground plane backing on the dielectric substrate (Figure 2 on page 2a), has led to interest in conductor backed coplanar (CBCP) line, which can be integrated compatibly on the same substrate with microstrip (Figure 2 on page 2b). The CBCP line is also sometimes called conductor backed coplanar waveguide (CBCPW).

The ground plane of CBCPW adds strength to a semiconductor chip used in microwave integrated circuit construction and provides a low loss ground return at microwave frequencies. The conductor backed coplanar line is the principal object of the present research. To date, only very limited literature reports have been published on the

transmission line parameters (characteristic impedance Z_0 and effective dielectric constant ϵ_{eff}) [Ref. 5 , 6].

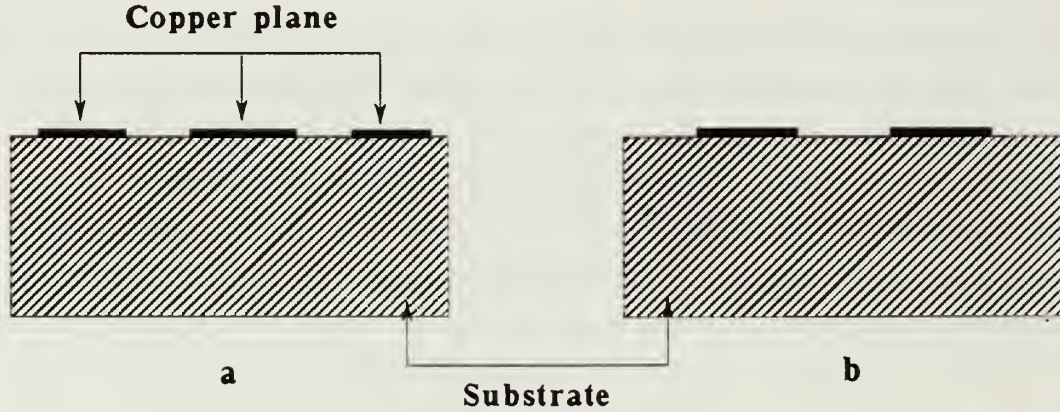


Figure 1. Coplanar systems

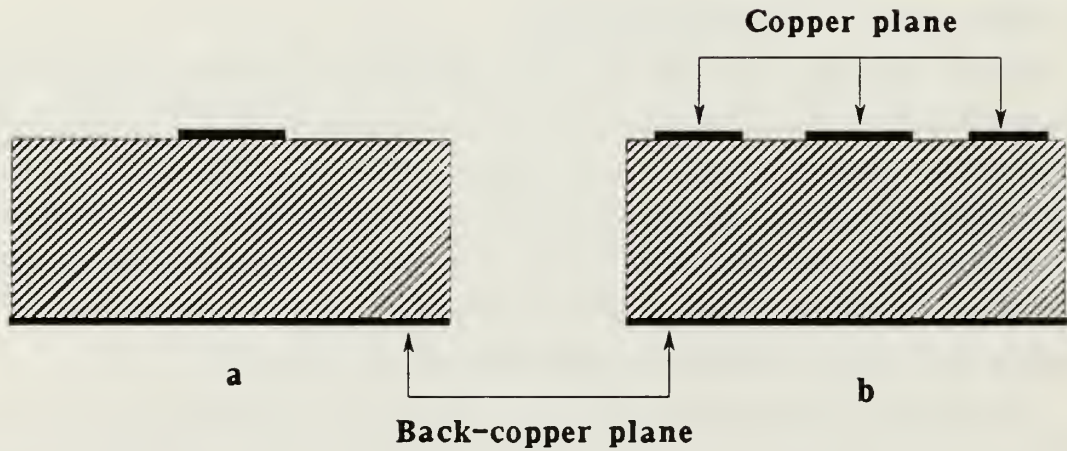


Figure 2. Conductor backed planar waveguides

In the present work only the TEM dominant low frequency propagation mode of coplanar line will be considered. The Transverse Electric (TE) and Transverse Magnetic (TM) hybrid modes which can propagate on planar systems will not be considered. The restriction to the assumed TEM mode has been employed in numerous investigations

of microstrip and other planar systems, and has been found to provide useful transmission parameters at frequencies up to 10 GHz.

An additional characteristic of propagation on multiconductor transmission systems is that odd and even modal excitations may propagate, resulting in undesired terminal characteristics for the line. The current flow characteristics of the dominant TEM mode, and a principal even mode are shown in Figure 3. Suppression of the unwanted modes is normally possible through adequate ground terminations for the coplanar ground planes, and care with the input excitation of the line.

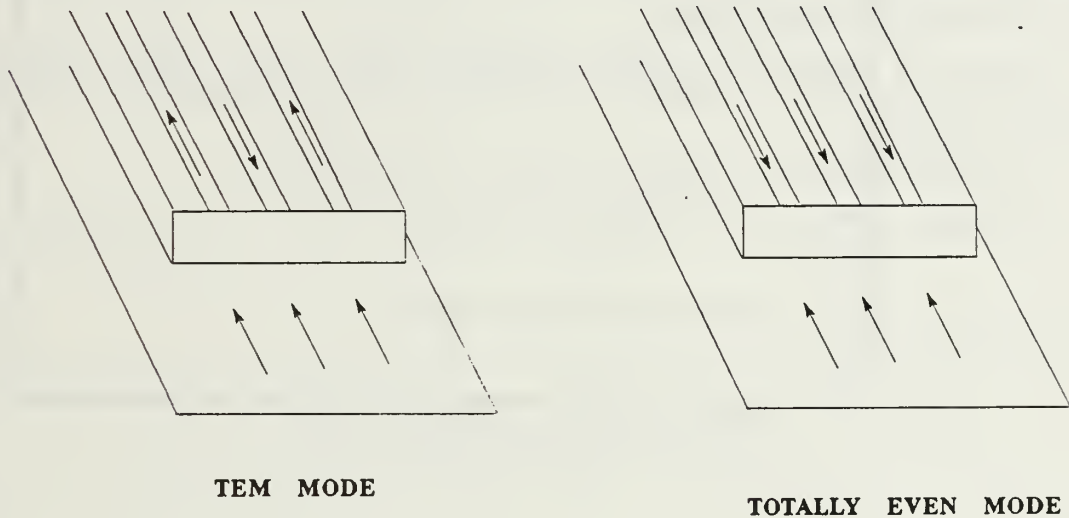


Figure 3. Current flow characteristics of propagation modes

II. ANALYSIS OF TEM PROPAGATION MODE

A. REVIEW OF ROWE & LAO BOUNDARY POINT MATCHING METHOD

In this section, the boundary point matching method for a CBCPW, which was presented by Rowe and Lao [Ref. 7], is reviewed, and the impedance (Z_0) and the effective dielectric constant (ϵ_{eff}) for the conductor backed coplanar line on a dielectric substrate are calculated. The coordinates employed in the analysis are given in Figure 4 on page 5. The line is assumed to be enclosed in a shielded enclosure of width $2l$, open at the top. The enclosure width will be taken to be large enough to cause negligible perturbation of the line fields.

To find the solution of Laplace's equation, define the two regions shown in Figure 4 on page 5:

1. The lower region is x, y coordinate system (in the dielectric).
2. The upper region is x', y' coordinate system (in air).

The solution of Laplace's equation in the upper region is:

$$\phi^+(x', y') = \sum_{i=1}^{\infty} a_i \cos(k_i x') \exp(-k_i y') \quad (1)$$

where,

$$k_i = \frac{(2i-1)\pi}{2l} \quad (2)$$

$$l = \frac{C}{2} + D \quad (3)$$

Assuming width D equal to $C/2$ produces negligible effect on the calculated parameters. The solution of Laplace's equation in the lower region is:

$$\phi^-(x, y) = \sum_{i=1}^{\infty} b_i \cos(k_i x) \sinh(k_i y) \quad (4)$$

The boundary conditions at the surface of the dielectric are:

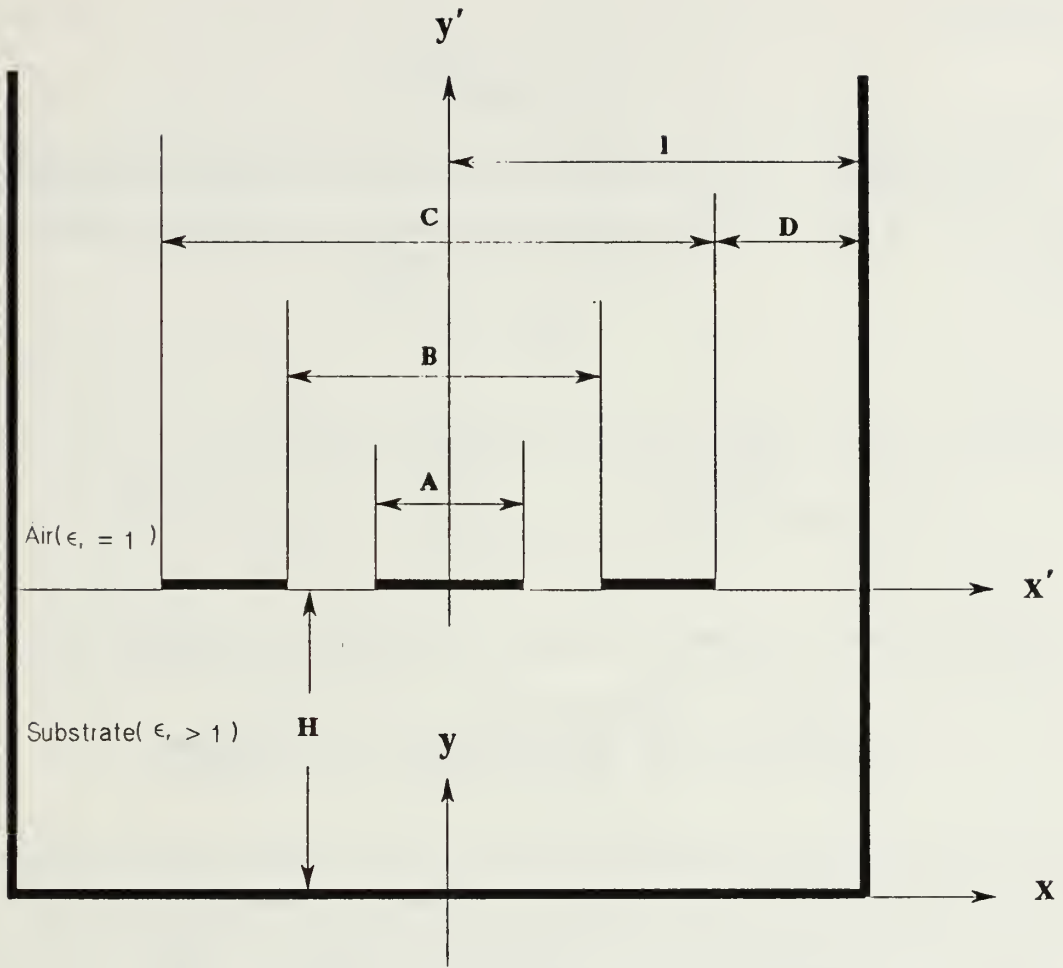


Figure 4. Geometry of a conductor backed CPW

$$\phi^+(0,0) = \sum_{i=1}^{\infty} a_i \quad (5)$$

$$\phi^-(0,H) = \sum_{i=1}^{\infty} b_i \sinh(k_i H) \quad (6)$$

$$\phi^+(0,0) = \phi^-(0,H) \quad (7)$$

therefore,

$$a_i = b_i \sinh(k_i H) \quad (8)$$

In the gap ($\frac{A}{2} < x < \frac{B}{2}$) between the conductors, and outside of the ground conductor ($\frac{C}{2} < x \leq l$), the surface normal component of the displacement field is continuous.

$$D_n^+ = D_n^- \quad (9)$$

where,

$$D_n = \epsilon \frac{\partial \phi}{\partial y} \quad (10)$$

Apply the boundary condition at the surface of the substrate to equations (9) and (10).

$$\epsilon_0 \frac{\partial \phi^+}{\partial y'} \bigg|_{y'=0} = \epsilon_r \epsilon_0 \frac{\partial \phi^-}{\partial y} \bigg|_{y=H}, \quad b_i = \frac{a_i}{\sinh(k_i H)} \quad (11)$$

therefore,

$$\sum_{i=1}^{\infty} a_i \cos(k_i x) \{1 + \epsilon_r \coth(k_i H)\} = 0, \quad \begin{cases} \frac{A}{2} < x < \frac{B}{2} \\ \frac{C}{2} < x \leq l \end{cases} \quad (12)$$

where ϵ_r = relative dielectric constant of substrate.

Generally the voltage on the inner conductor is set to unity so that the conductor capacitance is numerically equal to the charge on this conductor. The unity potential on the center conductor and the zero potential on the outer conductors lead to

$$\sum_{i=1}^{\infty} a_i \cos(k_i x) = \begin{cases} 1, & x \leq \frac{A}{2} \\ 0, & \frac{B}{2} \leq x \leq \frac{C}{2} \end{cases} \quad (13)$$

The above Fourier summations are terminated at $i=N$ to make problem suitable for numerical analysis. To find the N unknown a_i 's, x takes on N discrete values on the dielectric-air interface; at coordinates:

$$x_j = \frac{jl}{N+1}, \quad j = 1, 2, \dots, N \quad (14)$$

Equation (12) and (13) for the a_i 's can then be written as an N by N matrix equation.

$$\sum_{i=1}^N m_{ji} a_i = d_j, \quad j = 1, 2, \dots, N \quad (15)$$

where,

$$m_{ji} = \begin{cases} k_i \cos(k_i x_j) \{1 + \epsilon_r \coth(k_i h)\}, & \frac{A}{2} < x_j < \frac{B}{2}, \quad \frac{C}{2} < x_j \leq l \\ \cos(k_i x_j), & x_j \leq \frac{A}{2}, \quad \frac{B}{2} \leq x_j \leq \frac{C}{2} \end{cases} \quad (16)$$

and

$$d_j = \begin{cases} 1, & x_j \leq \frac{A}{2} \\ 0, & x_j > \frac{A}{2} \end{cases} \quad (17)$$

The matrix equation (15) is solved by Gaussian elimination to find the a_i 's.

In order to compute the impedance, the capacitance per unit length of guide from the center conductor to ground is calculated by integrating the normal component of D-field on a Gaussian surface enclosing the center conductor only. Figure 5 on page 8 shows the surface S chosen for the integration. The capacitance is:

$$C = \epsilon_0 \int_S \epsilon_r \vec{E} d\vec{S} = -\epsilon_0 \int_S \epsilon_r \vec{\nabla} \phi d\vec{S} \quad (18)$$

therefore,

$$C = -2\epsilon_0 \sum_{i=1}^N a_i \sin(k_i \frac{A+B}{4}) \{1 + \epsilon_r \coth(k_i H)\} \quad (19)$$

where $\epsilon_0 = \frac{10^{-9}}{36\pi} = 8.84 \times 10^{-12}$

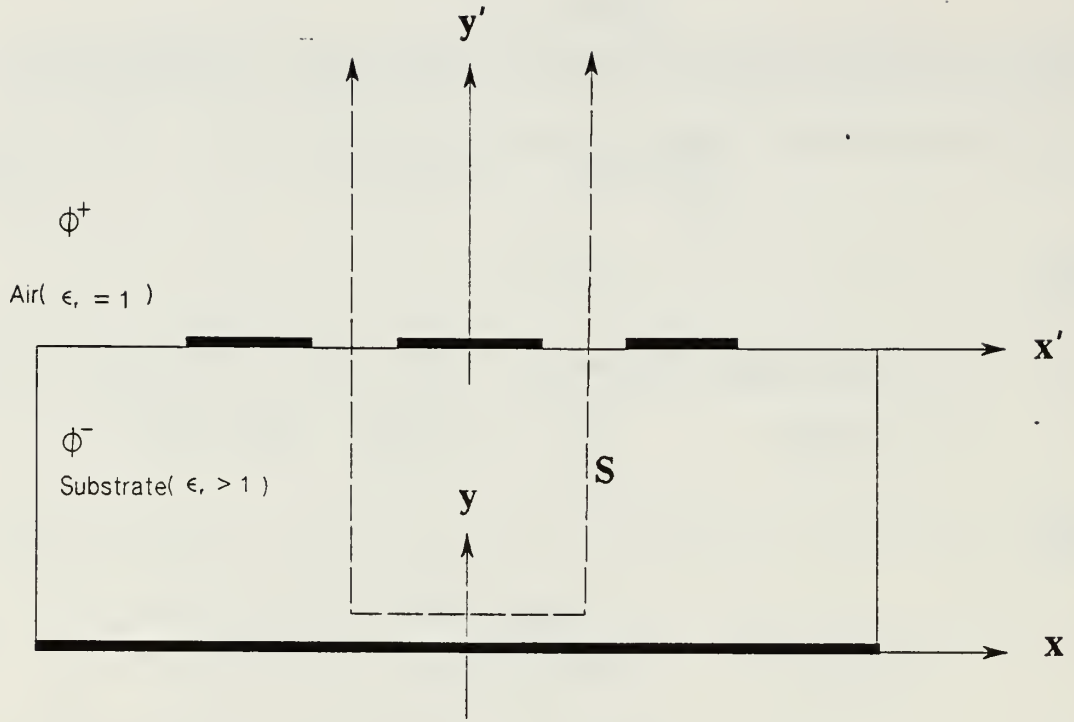


Figure 5. Gaussian surface in the capacitance calculation

The static impedance and effective dielectric constant can be calculated from standard TEM-modal relations:

$$Z_0 = \frac{1}{v\sqrt{CC_0}} \quad (20)$$

and

$$\epsilon_{\text{reff}} = \frac{C}{C_0} \quad (21)$$

where $v = 3 * 10^8$ m/s, C is the capacitance with the dielectric layer present, and C_0 is the capacitance when the dielectric is replaced by air.

Figure 6 on page 9 and Figure 7 on page 10 show the calculated results of impedance and effective dielectric constant of CBCPW using boundary point matching method.

ROWE AND LAO METHOD IMPEDANCE

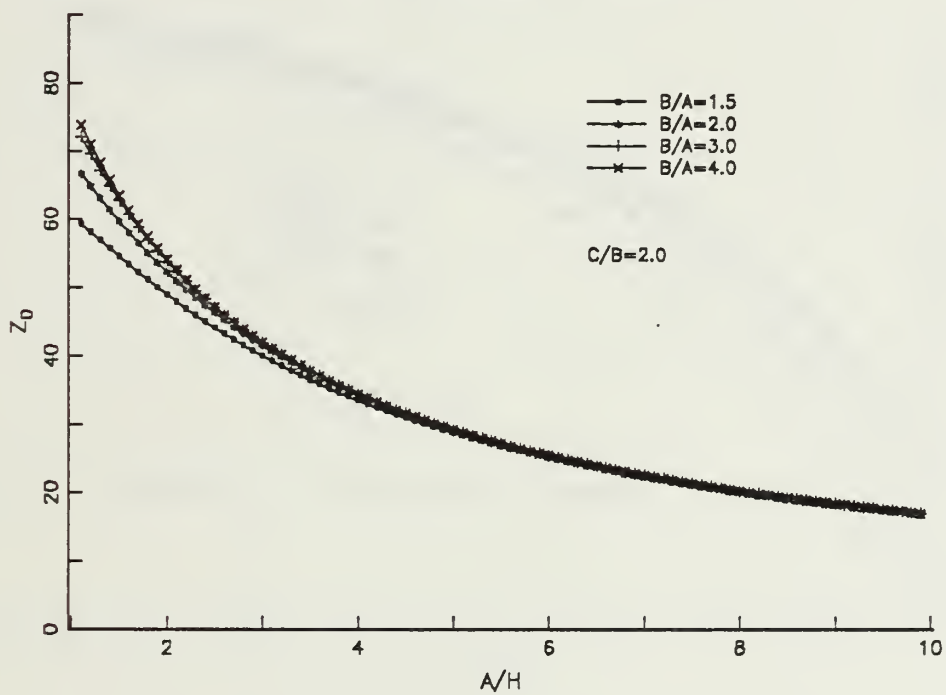


Figure 6. Calculated characteristic impedance of CBCPW by boundary point matching method: ($\epsilon_r = 3.52$, $H = 1.5$ mm)

ROWE AND LAO METHOD
EFFECTIVE DIELECTRIC CONSTANT

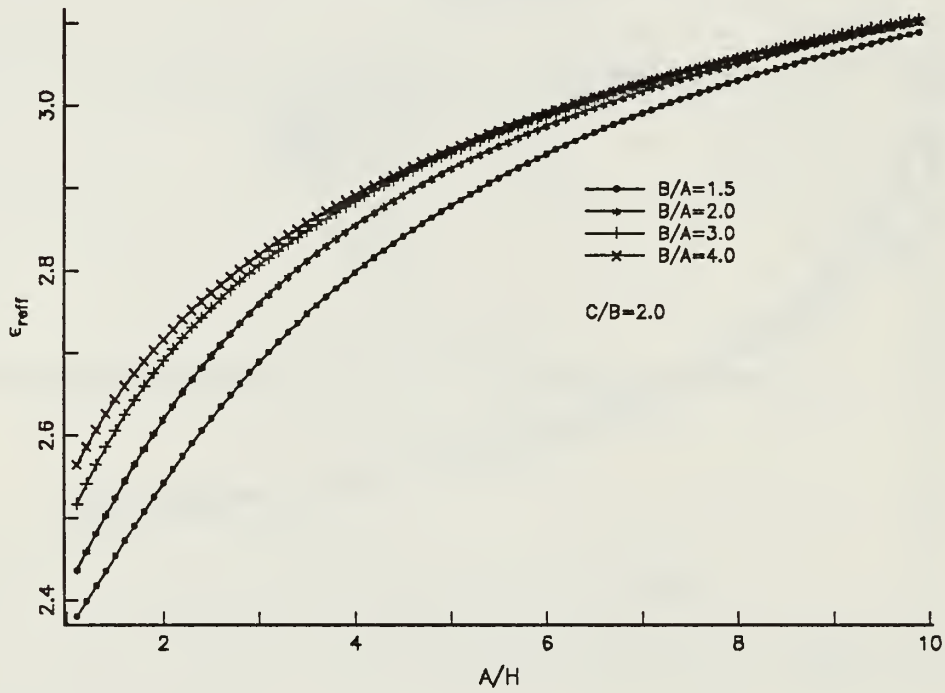


Figure 7. Calculated effective dielectric constant of CBCPW by boundary point matching method: ($\epsilon_r = 3.52$, $H = 1.5$ mm)

B. REVIEW OF YAMASHITA'S VARIATIONAL METHOD

A method for computing impedance (Z_0) and effective dielectric constant (ϵ_{eff}) of conductor backed coplanar waveguide is based on the application of Fourier transform and variational techniques [Ref. 8]. Figure 8 shows the geometry of CBCPW for variational method.

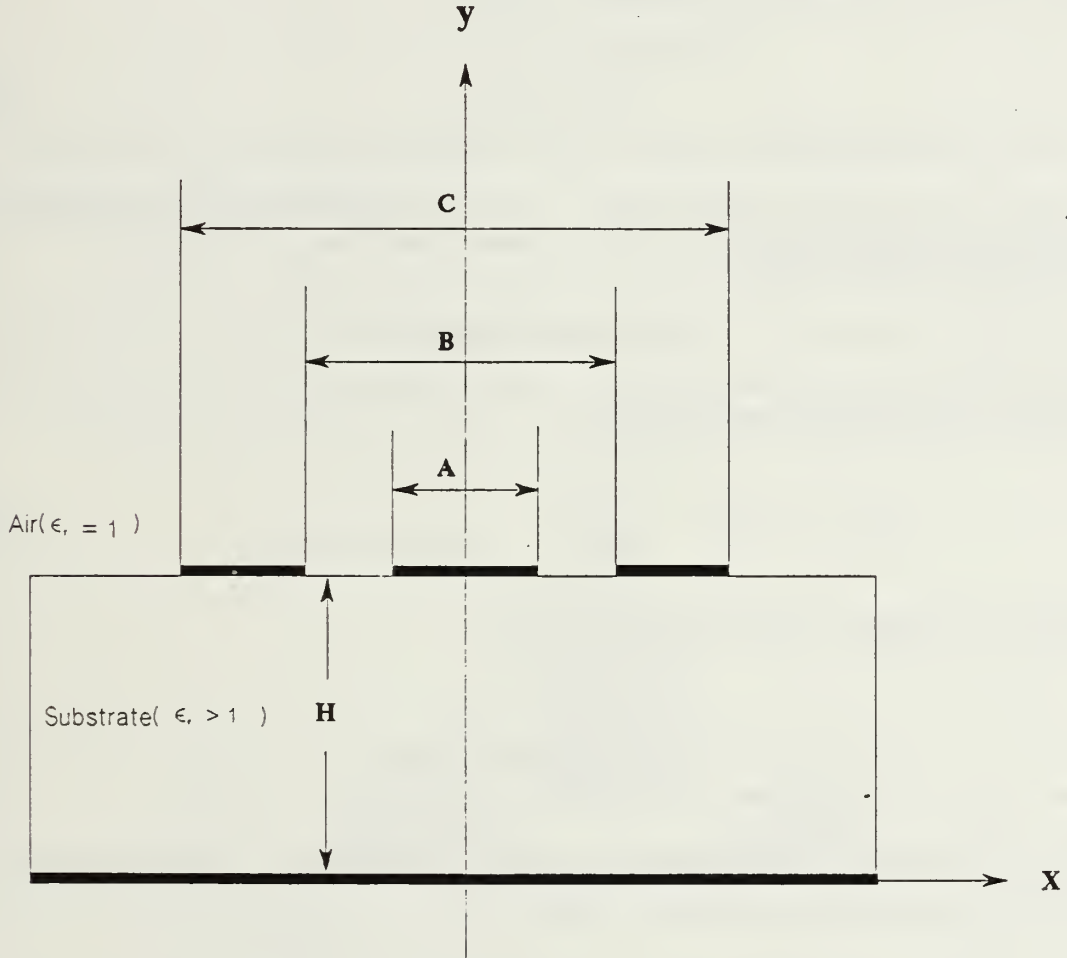


Figure 8. Geometry of CBCPW

The static potential distribution $\phi(x,y)$ in the planar line structure satisfies Poisson's equation:

$$\nabla^2 \phi(x,y) = -\frac{1}{\epsilon} \rho(x,y) \quad (22)$$

where $\rho(x,y)$ is charge distribution on the surface of the conducting strips.

A variational expression for the line capacitance is:

$$C = \frac{Q^2}{\int_s \rho(x,y) \phi(x,y) dl} \quad (23)$$

where Q is the total charge per unit length of strip:

$$Q = \int_x \rho(x) dx \quad (24)$$

We assume that the strip is infinitely thin. For the infinitely thin strip case, the charge distribution assumes the form

$$\rho(x,y) = f(x) \delta(y - H) \quad (25)$$

where $f(x)$ is even function and $\delta(y - H)$ is:

$$\delta(y - H) = \begin{cases} 1, & y = H \\ 0, & y \neq H \end{cases} ; \text{ Dirac's } \delta \text{ function.} \quad (26)$$

Now define the Fourier transform $\tilde{\phi}(\beta, y)$ of $\phi(x, y)$.

$$\tilde{\phi}(\beta, y) = \int_{-\infty}^{\infty} \phi(x, y) e^{j\beta x} dx \quad (27)$$

With use of the known Green's function for this problem [Ref. 9], the Fourier transform of the potential distribution at $y = H$ is:

$$\tilde{\phi}(\beta, H) = \frac{\tilde{f}(\beta)}{\epsilon_0 |\beta| \{1 + \epsilon_r \coth(|\beta| H)\}} \quad (28)$$

$$C = \frac{2\pi Q^2}{\int_{-\infty}^{\infty} \tilde{f}(\beta) \tilde{\phi}(\beta, H) d\beta} \quad (29)$$

Insert the equation (28) into (29), then the final variational expression is:

$$C = \frac{\pi \epsilon_0 Q^2}{\int_0^\infty \frac{\{\tilde{f}(\beta)\}^2}{\{1 + \epsilon_r \coth(\beta H)\} \beta} d\beta} \quad (30)$$

where,

$$\tilde{f}(\beta) = \int_x f(x) e^{j\beta x} dx \quad (31)$$

where $f(x)$ is the density distribution of the charge on the strips, and symmetry with respect to $x=0$ is assumed.

As shown in Figure 9 and Figure 10, two forms of elementary charge distribution on the center conductor, $f(x) = \text{constant}$ and $f(x) = |x|$, were tested. The negative charge on the two ground-plane conductors is assumed to be constant in both cases. The computation was found to be insensitive to the form assumed for the charge distribution on the top ground planes, hence the uniform (negative) charge distribution was assumed.

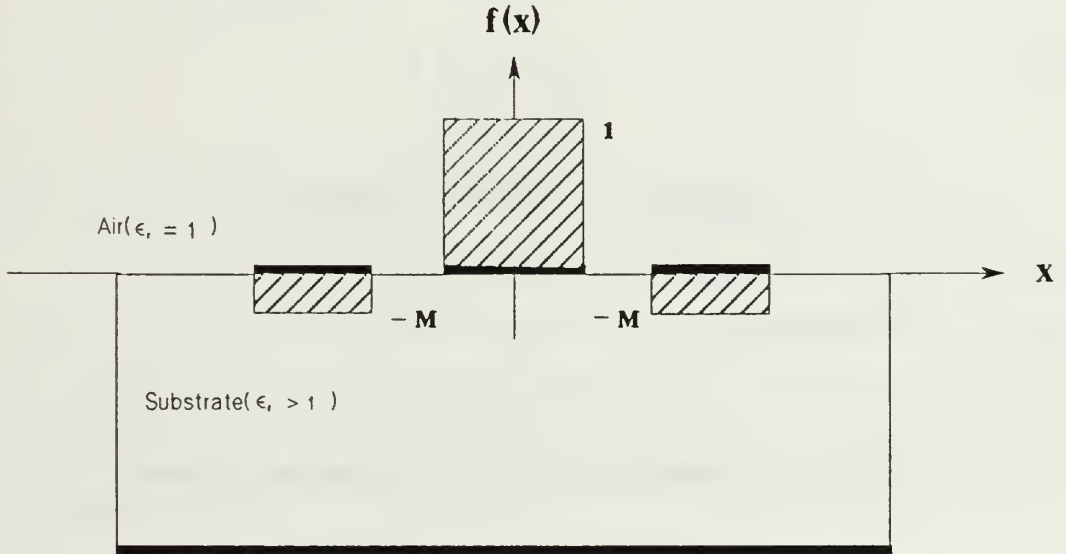


Figure 9. Assumed step-charge density function of CBCPW: ($f(x) = \text{constant}$)

In case of Figure 9 on page 13, the assumed elementary charge distribution function is:

$$f(x) = \begin{cases} 1, & -\frac{A}{2} \leq x \leq \frac{A}{2} \\ -M, & \frac{B}{2} \leq |x| \leq \frac{C}{2} \\ 0, & \text{otherwise} \end{cases} \quad (32)$$

The Fourier transform of $f(x)$ is:

$$\tilde{f}(\beta) = \frac{2}{\beta} \left[\sin(\beta \frac{A}{2}) + M \left\{ \sin(\beta \frac{B}{2}) - \sin(\beta \frac{C}{2}) \right\} \right] \quad (33)$$

and,

$$Q = A + M(B - C) \quad (34)$$

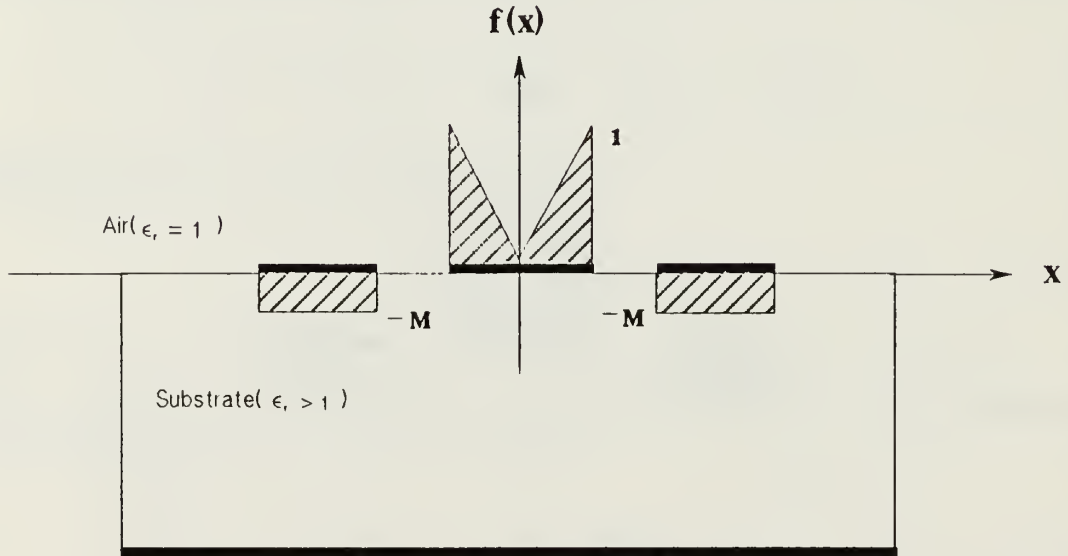


Figure 10. Assumed linear-charge density function of CBCPW: $(f(x) = |x|)$

In case of Figure 10, the assumed elementary charge distribution function is:

$$f(x) = \begin{cases} |x|, & -\frac{A}{2} \leq x \leq \frac{A}{2} \\ -M, & \frac{B}{2} \leq |x| \leq \frac{C}{2} \\ 0, & \text{otherwise} \end{cases} \quad (35)$$

The Fourier transform of $f(x)$ is:

$$\tilde{f}(\beta) = Q \left[\frac{2 \sin(\beta \frac{A}{2})}{\beta \frac{A}{2}} - \left\{ \frac{\sin(\beta \frac{A}{4})}{\beta \frac{A}{4}} \right\}^2 \right] + \frac{2M}{\beta} \left\{ \sin(\beta \frac{B}{2}) - \sin(\beta \frac{C}{2}) \right\} \quad (36)$$

and,

$$Q = \frac{A}{2} + M(B - C) \quad (37)$$

The characteristic impedance is:

$$Z_0 = \frac{1}{v \sqrt{CC_0}} \quad (38)$$

$$\epsilon_{\text{eff}} = \frac{C}{C_0} \quad (39)$$

where $v = 3 \times 10^8$ m/s, and C_0 is calculated by setting $\epsilon_r = 1$.

The variational expression with the elementary charge distribution function $f(x) = |x|$, is found to be the one that maximizes the value of capacitance C , thus giving the closest value to the exact result for the capacitance. In the simple distributions chosen, M is the variational parameter, and maximum capacitance C is found by reducing M to a low value (see page 18). Figure 11 on page 16 and Figure 12 on page 17 show the calculated results of impedance and effective dielectric constant of CBCPW using variational method.

VARIATIONAL METHOD
IMPEDANCE

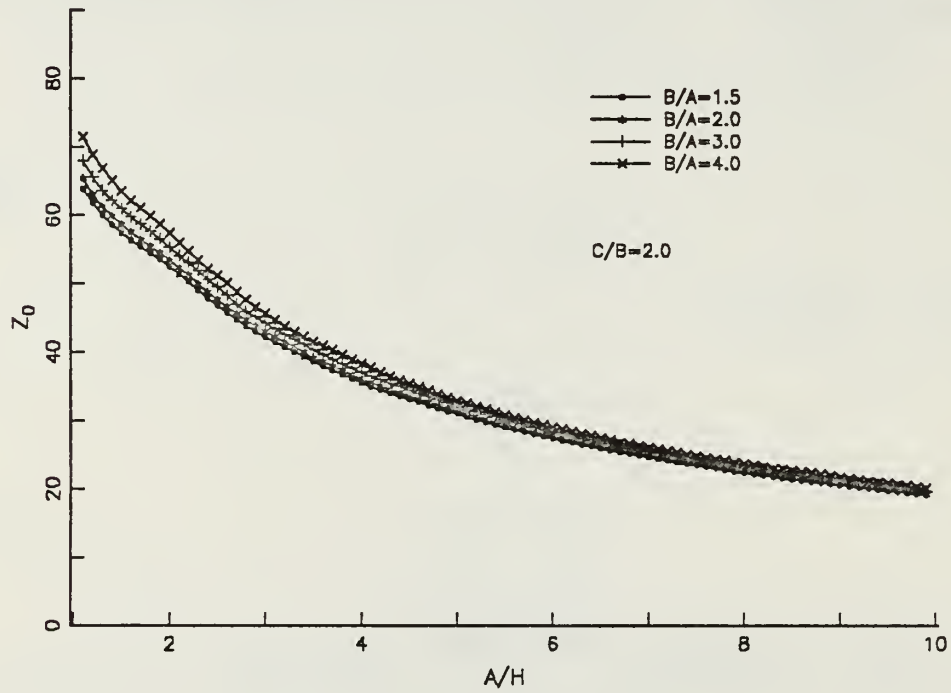


Figure 11. Calculated characteristic impedance of CBCPW by variational method: ($\epsilon_r = 3.52$, $H = 1.5$ mm)

VARIATIONAL METHOD
EFFECTIVE DIELECTRIC CONSTANT

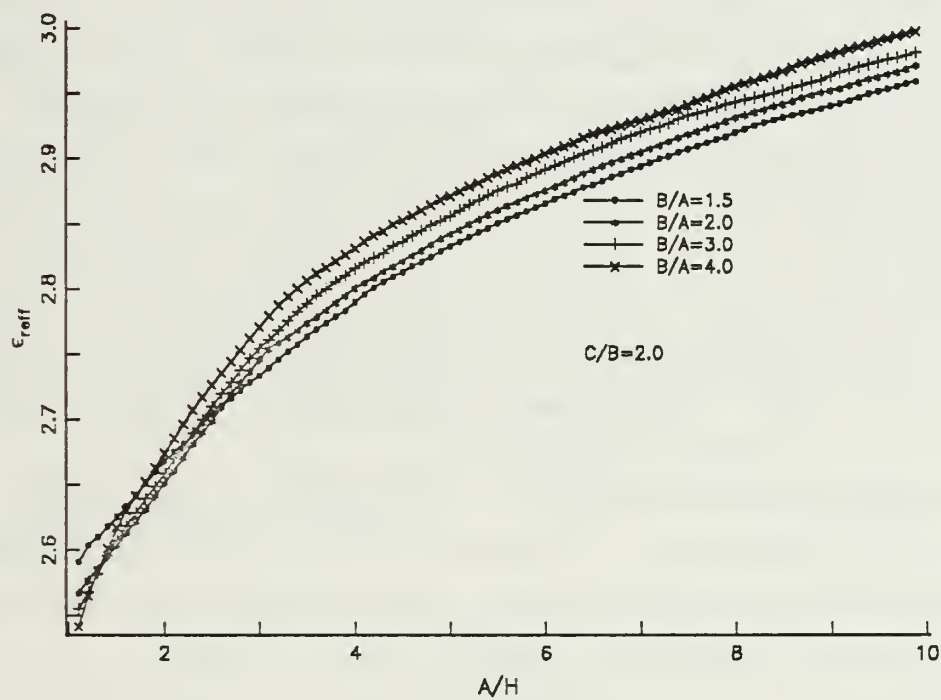


Figure 12. Calculated effective dielectric constant of CBCPW by variational method: ($\epsilon_r = 3.52$, $H = 1.5$ mm)

C. COMPARISON OF RESULTS

A coplanar waveguide consists of a strip of thin metallic film on the surface of a dielectric slab with two ground electrodes running adjacent and parallel to the strip. Two methods, the boundary point matching method and the variational method, were used to calculate the effective dielectric constant (ϵ_{eff}) and impedance (Z_0) as a function of the line dimensions.

The calculated impedance and effective dielectric constant of conductor backed coplanar waveguide are shown in Figures 6, 7, 11 and 12. To compare the results of the boundary point matching method and variational method, several graphs are plotted (Figure 13 on page 20 through Figure 20 on page 27) for various line parameters.

In the case of the Rowe and Lao boundary point matching method calculation, the impedance and effective dielectric constant are computed by choosing the number of matching-points, N , equal to 100. The accuracy of this computation increases with N , but the computation time of the N by N matrix increases approximately as N^4 . A value of $N = 100$ is chosen in the present work, for a moderate computation time and acceptable accuracy of the results. Choice of larger N leads to roundoff errors and excessive computation time in the matrix calculation.

The characteristic impedance increases as the center conductor width decreases and decreases as the slot widths decrease. As shown by the Rowe and Lao boundary point matching method, when the aspect ratio $A/H \geq 5$ the slot width ratio has small effect on the impedance values. This behavior is shown in Figure 6 on page 9.

For a large aspect ratio A/H versus the ratio of B/A , the impedance (Z_0) does not change much, since both the slot coupling effect and the effect of the ground backing are small. This shows that characteristic impedance (Z_0) reflects the coupling effect between the two slots. Therefore, by adjusting both slot widths and center conductor width, independent control of the characteristic impedance can be obtained. For the Rowe and Lao boundary point matching method, the effective dielectric constant increases as the center strip width increases and decreases as the slot widths decrease.

It is interesting to note that the effective dielectric constant ϵ_{eff} of CBCPW approaches microstrip behavior in its dependence on the linewidth ratio A/H , especially for wide slots ($B/A = 4.0$ in Figure 7 on page 10). For microstrip, as microstrip line ratio A/H goes to zero, its value of ϵ_{eff} approaches $\frac{\epsilon_r + 1}{2} = 2.26$, in this case, and as A/H goes to ∞ , then ϵ_{eff} goes to ϵ_r . Similar behavior is also noted for CBCPW in Figure 7 on page 10.

In case of Yamashita's variational method, the impedance and the effective dielectric constant are calculated using a value of $M = 0.04$. The ratio of the charge density magnitude value between the center strip and outer strip is thus in the range 20:1 - 50:1. The impedance and the effective dielectric constant are compared with the Rowe and Lao results by calculation using the same parameters.

The results from the variational method are in good agreement with those of the Rowe & Lao method. For impedance, Figure 13 on page 20 through Figure 16 on page 23 shows that less than 6% difference in Z_0 was observed for most cases, and also Figure 17 on page 24 through Figure 20 on page 27 shows less than 5% deviation in the effective dielectric constant values. The outputs of the both methods are closer as the slot widths increase. The characteristics approach those of microstrip as the slot widths increase and the ground planes have less effect. For example, microstrip lines on this substrate having linewidth ratios A/H equal to 1 and 10 would have characteristic impedances Z_0 equal to 78.7 ohms and 16.6 ohms, respectively, and effective dielectric constant ϵ_{eff} of 2.61 and 3.13, respectively. These are comparable to the wide-slot values ($B/A = 4.0$) for CBCPW seen in Figures 16 and 20. The computation time on the IBM 3278 for one data point is:

- Boundary point matching method = 50 sec.
- Variational method = 10 sec.

COMPARISON OF METHODS
IMPEDANCE

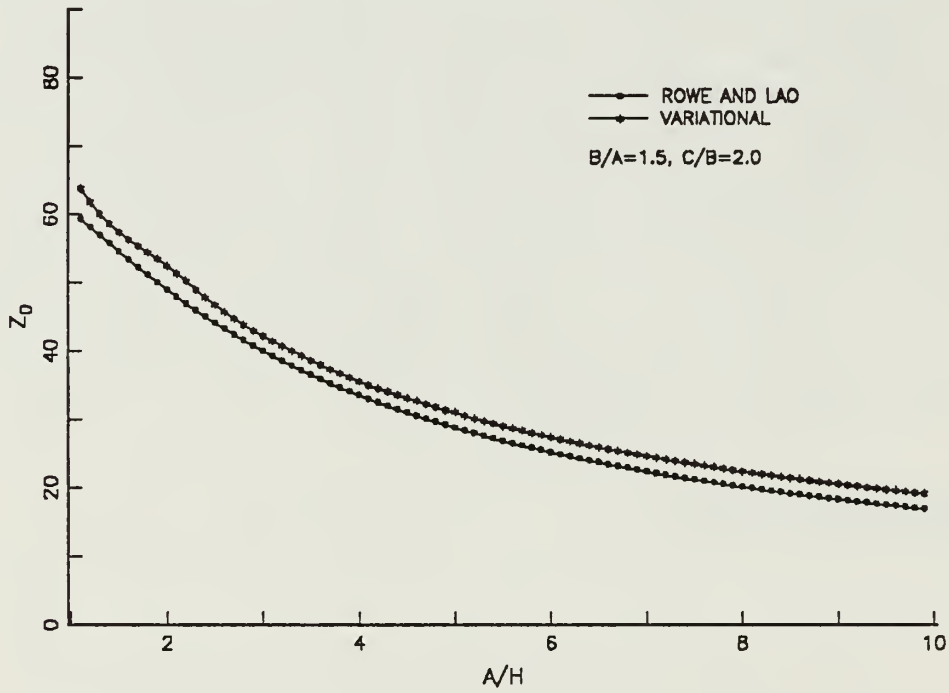


Figure 13. Computed results for characteristic impedance versus strip width with line dimensions as parameters: ($B/A = 1.5$, $C/B = 2.0$, $\epsilon_r = 3.52$, $H = 1.5 \text{ mm}$)

COMPARISON OF METHODS IMPEDANCE

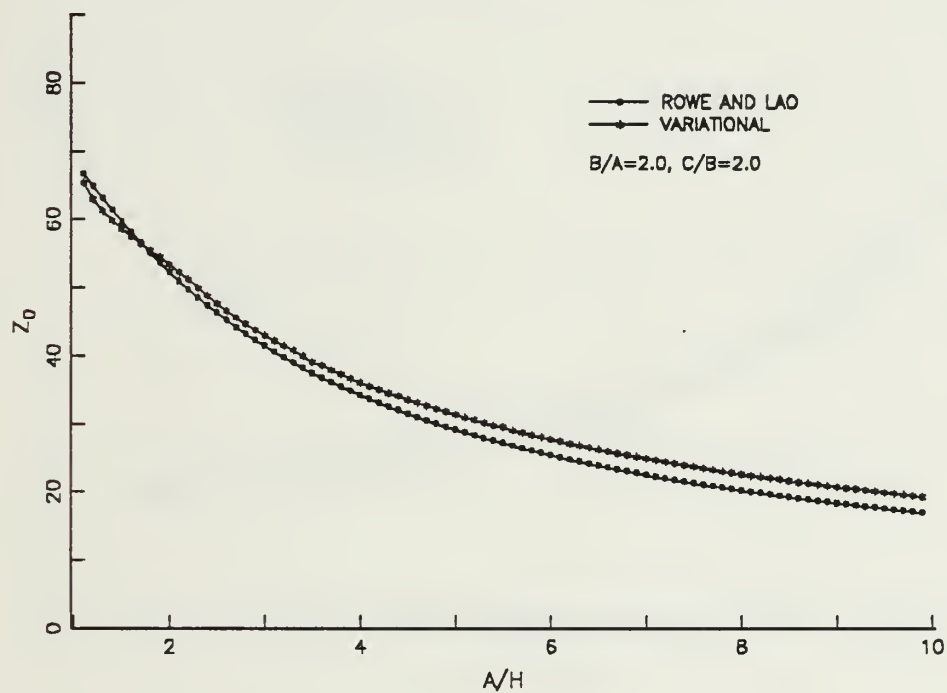


Figure 14. Computed results for characteristic impedance versus strip width with line dimensions as parameters: ($B/A = 2.0$, $C/B = 2.0$, $\epsilon_r = 3.52$, $H = 1.5 \text{ mm}$)

COMPARISON OF METHODS IMPEDANCE

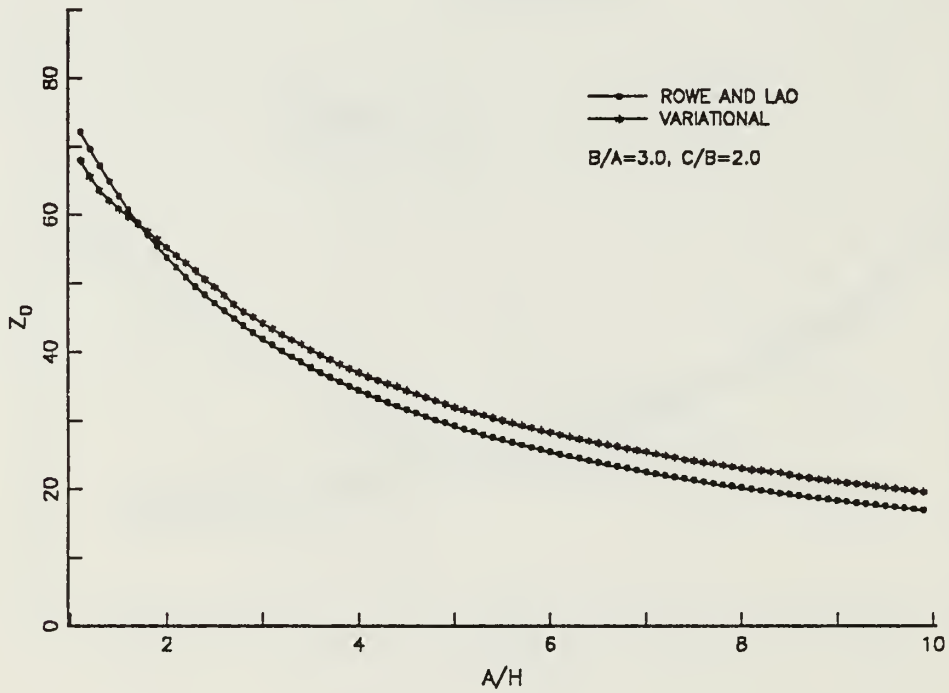


Figure 15. Computed results for characteristic impedance versus strip width with line dimensions as parameters: ($B/A = 3.0$, $C/B = 2.0$, $\epsilon_r = 3.52$, $H = 1.5 \text{ mm}$)

COMPARISON OF METHODS
IMPEDANCE

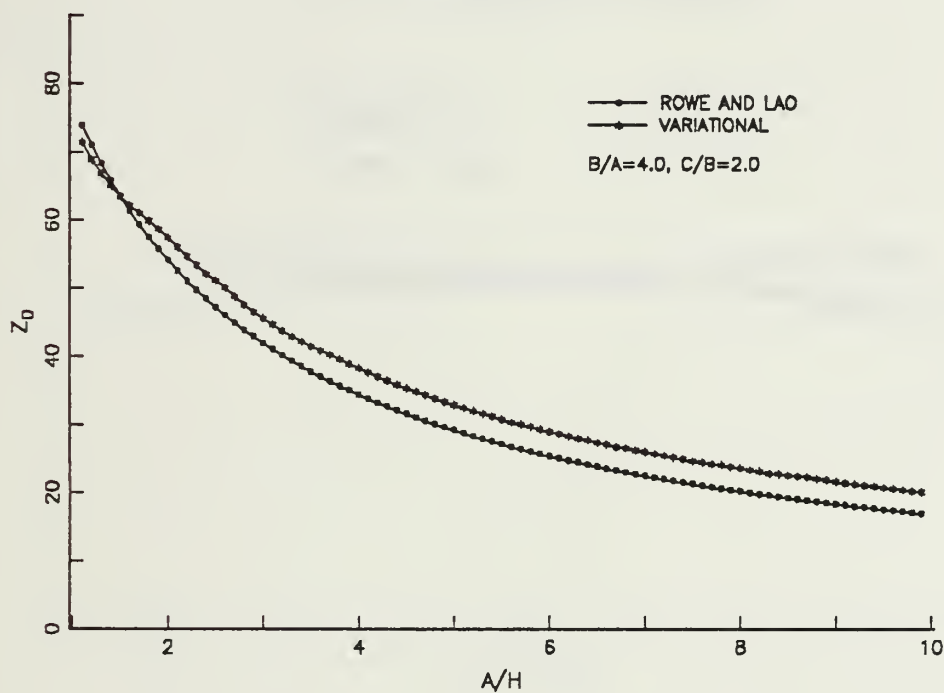


Figure 16. Computed results for characteristic impedance versus strip width with line dimensions as parameters: ($B/A=4.0, C/B=2.0, \epsilon_r = 3.52, H = 1.5 \text{ mm}$)

COMPARISON OF METHODS EFFECTIVE DIELECTRIC CONSTANT

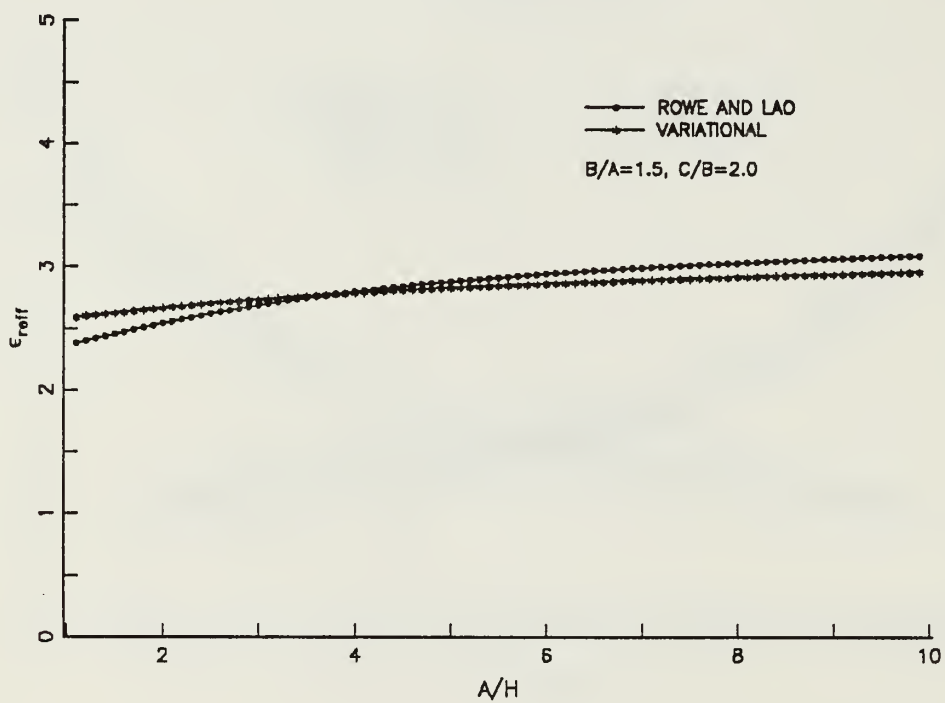


Figure 17. Computed results for dielectric constant versus strip width for various line parameters: ($B/A=1.5$, $C/B=2.0$, $\epsilon_r = 3.52$, $H = 1.5$ mm)

COMPARISON OF METHODS
EFFECTIVE DIELECTRIC CONSTANT

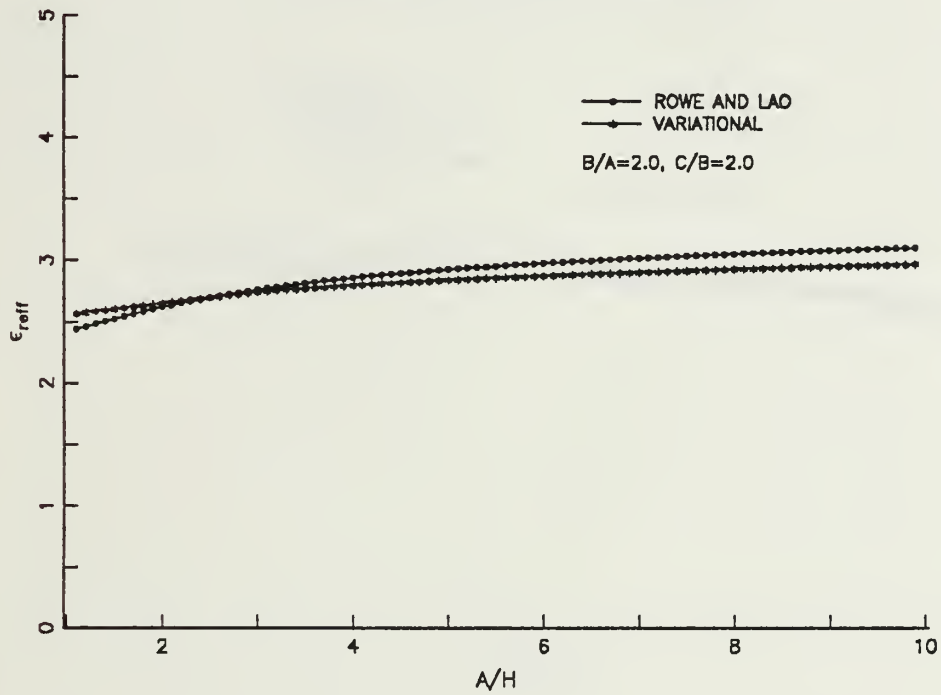


Figure 18. Computed results for dielectric constant versus strip width for various line parameters: ($B/A = 2.0$, $C/B = 2.0$, $\epsilon_r = 3.52$, $H = 1.5$ mm)

COMPARISON OF METHODS
EFFECTIVE DIELECTRIC CONSTANT

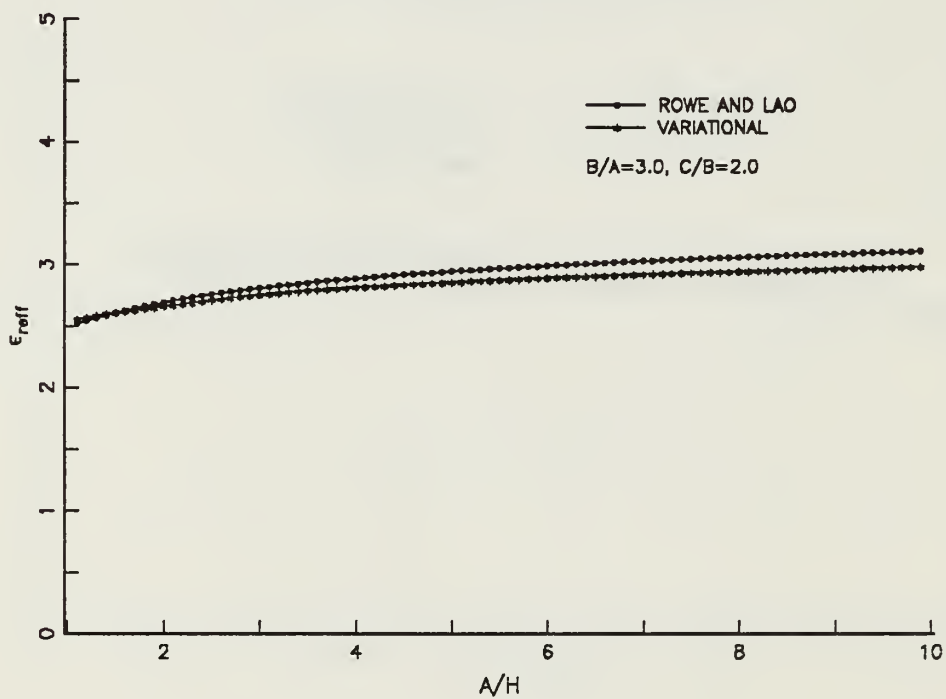


Figure 19. Computed results for dielectric constant versus strip width for various line parameters: ($B/A = 3.0$, $C/B = 2.0$, $\epsilon_r = 3.52$, $H = 1.5$ mm)

COMPARISON OF METHODS
EFFECTIVE DIELECTRIC CONSTANT

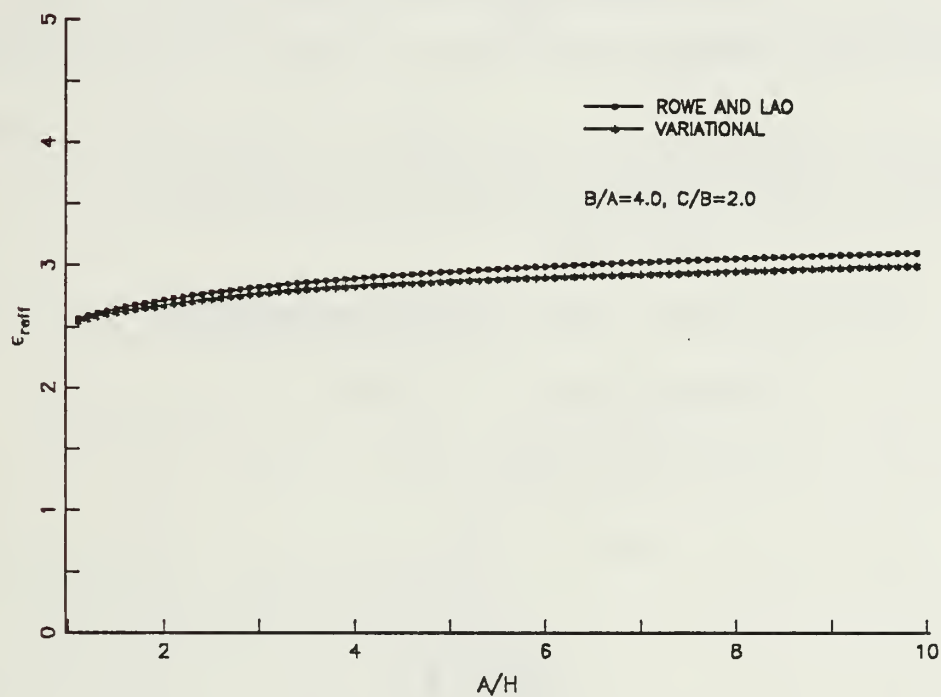


Figure 20. Computed results for dielectric constant versus strip width for various line parameters: ($B/A = 4.0$, $C/B = 2.0$, $\epsilon_r = 3.52$, $H = 1.5$ mm)

III. CONSTRUCTION OF COPLANAR LINES AND TRANSITIONS

A. ADHESIVE FOIL METHOD

In this section, the adhesive foil method for circuit fabrication is described. For the design of a coplanar line it is essential to have accurate knowledge of the dielectric constant of the substrate. An illustration of the use of adhesive foil in planar circuitry is in the measurement made to determine the substrate ϵ_r by means of a microstrip resonator circuit.

To measure the dielectric constant of substrate used in the present work, a quarter wave length stub of conventional microstrip is used as shown in Figure 21.

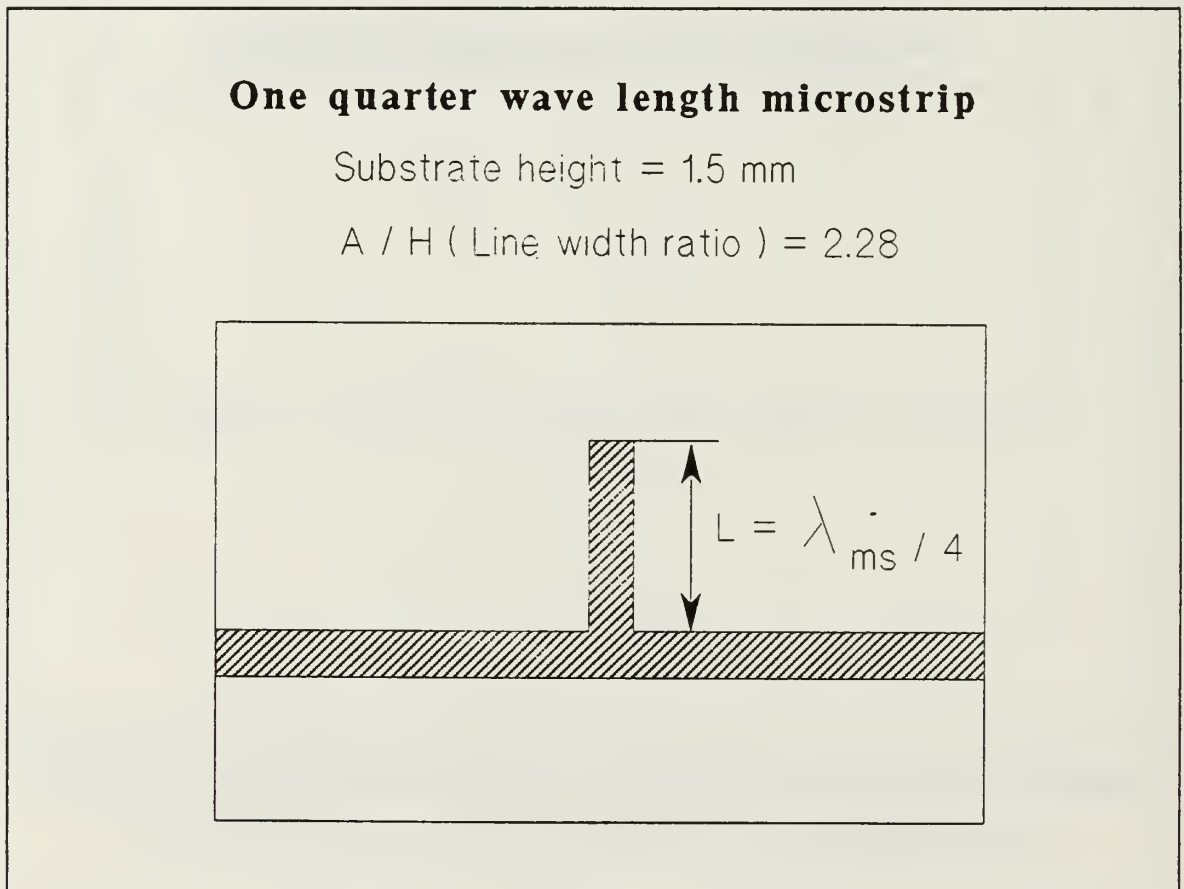


Figure 21. Quarter wave length stub for substrate dielectric constant measurement

The line pattern is fastened to the substrate using adhesive copper foil. The value of S_{21} or S_{12} , transmission coefficient, is measured with respect to frequency using the net-

work analyzer to find the resonant frequency, which occurs at maximum dB transmission loss (see Figure 22 on page 29).

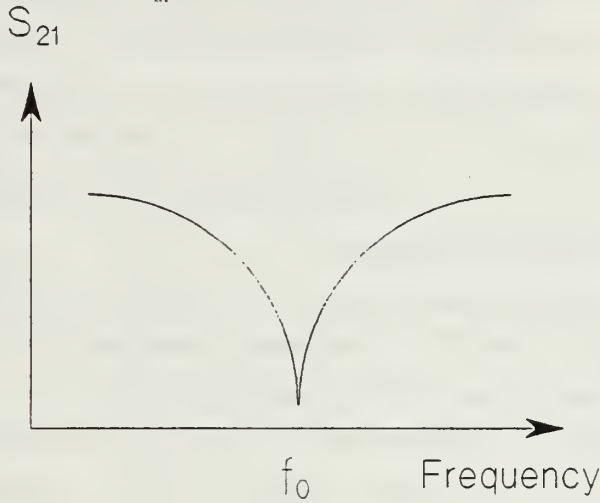


Figure 22. DB Magnitude plot for S_{21}

The following equations are used to find the dielectric constant of the substrate:

$$l = \frac{\lambda_{ms}}{4} \quad (\text{at } f_0) \quad (40)$$

$$\begin{aligned} v_{ms} &= f_0 \lambda_{ms} \\ &= \frac{c}{\sqrt{\epsilon_{rem}}} \end{aligned} \quad (41)$$

therefore,

$$\begin{aligned} \epsilon_{rem} &= \left(\frac{c}{f_0 \lambda_{ms}} \right)^2 \\ &= \left(\frac{c}{4lf_0} \right)^2 \\ &= \left(\frac{3 \times 10^8}{4 \times 0.03 \times 1.5 \times 10^9} \right)^2 \\ &= 2.8 \end{aligned} \quad (42)$$

where ϵ_{rem} is the microstrip value of effective dielectric constant on the substrate material employed. Using standard microstrip relations, the substrate relative dielectric constant was found to be: $\epsilon_r = 3.52$.

And next, with this dielectric constant (ϵ_r), the CBCPW parameters may be computed by using the Rowe and Lao method which is presented in the previous chapter, and the coplanar line may be constructed on the same substrate material.

The final steps for fabrication of CBCPW are the attachment of the line strips to a transition to coaxial line and soldering the outer conductors to ground with good connections, to reduce the insertion loss. In this adhesive foil method, the disadvantages are lack of precision and difficult assembly, since cutting and attaching is done manually.

B. PHOTOLITHOGRAPHICAL METHOD

To overcome the inaccuracy of the adhesive foil method, a photolithographical method for CBCPW design is used. This method employs a CAD program, photolithography and an etching process to form the line pattern.

Real-size design is possible on the computer by using the available CAD software tool with CBCPW parameters from the Rowe and Lao calculation. A real-size negative film is then made at the photo shop (This work was done at the NPS Educational Media Department). The exposure of the CBCPW pattern is done with this negative film. Figure 23 on page 31 shows drawn real-size line pattern and negative.

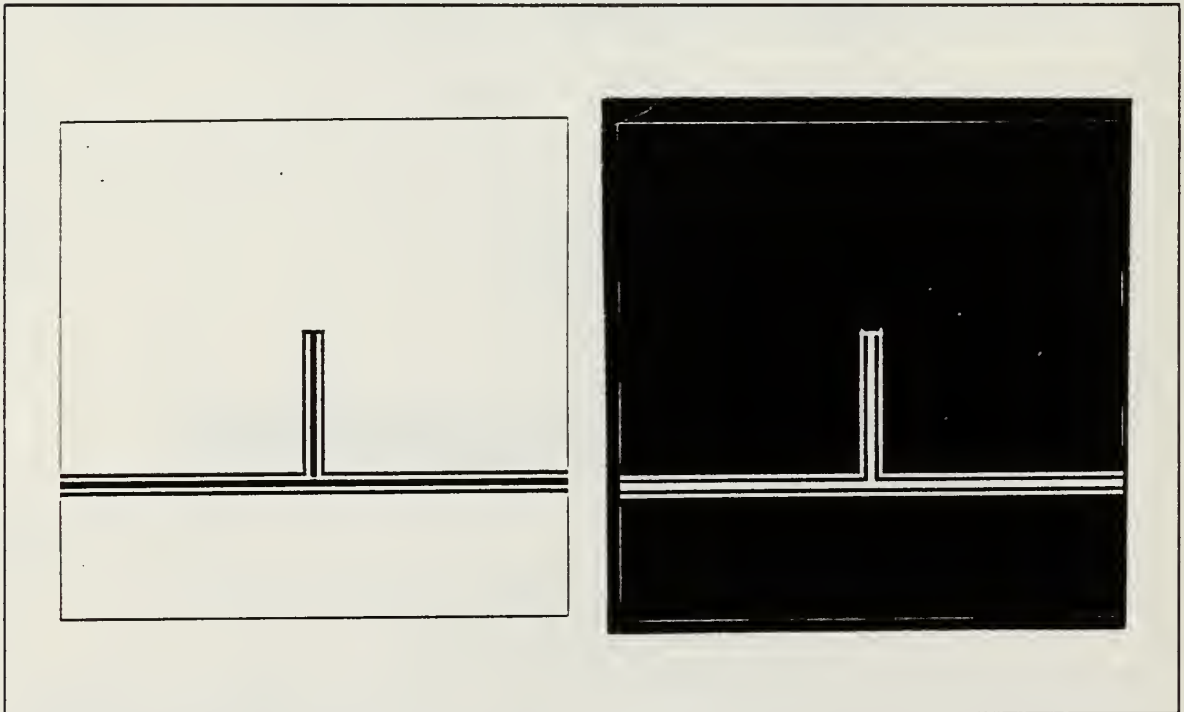


Figure 23. Drawn line pattern and negative

The circuit board etching process is:

1. Expose photosensitive emulsion through the prepared mask.
2. Allow board to run through the etcher to remove all unwanted copper.
3. After ensuring by visual inspection that all unwanted copper has been removed, remove negative film from board using acetone.

The advantage of this method is that greater precision is achieved than with the adhesive foil method.

C. TRANSITION TO COAXIAL LINE

It is necessary to make a transition from the CBCPW to a conventional transmission medium. An important factor in making such transitions is an impedance match and a field match. The field match, which is the prerequisite to a proper impedance match, is provided by the mechanical transition and the impedance match is provided by the electrical design. In this section, the mechanical transition of the CBCPW to coaxial line will be described.

The transition from a microstrip line to coaxial line is obtained by connecting the center pin of the coaxial connector to the microstrip. In contrast to the microstrip line, a conductor backed coplanar waveguide has ground conductors and a center conductor (signal line) on the one side of the substrate, and it also has a ground plane on the other side of the substrate. Therefore, the requirement of CBCPW transition to coaxial line is different than the microstrip case.

The CBCPW transition to coaxial line is obtained by extending the center pin of the coaxial connector to the center conductor of CBCPW to make signal contact, and by connecting the ground flange of the coaxial connector to outer conductor and back-plane of CBCPW. Therefore, top and bottom ground plane connectors are required to make a transition from a CBCPW to coaxial line.

The objective of the coaxial line to CBCPW transition is to obtain an impedance match and very low insertion loss. When attaching the coaxial connector to the CBCPW, it is essential to have a good contact which is as direct (short) as possible to reduce insertion loss. This requires careful mechanical design to conform to the geometry of the CBCPW.

A coupling unit was constructed to make the transition from CBCPW to N-type coaxial line. In addition to providing the connection from the coaxial center conductor to the CBCPW center conductor, a pair of tab connectors were provided at the top of the substrate so that soldered ground connections from the fixture to the two coplanar ground lines could be made.

IV. MEASUREMENT OF COPLANAR LINE PARAMETERS

A. RESONATOR METHOD FOR PHASE VELOCITY AND EFFECTIVE DIELECTRIC CONSTANT

In this section, two methods for calculating phase velocity and effective dielectric constant were explored. The first method used a series open-ended resonator; the second method used a shunt resonator.

1. Series Open-ended Resonator

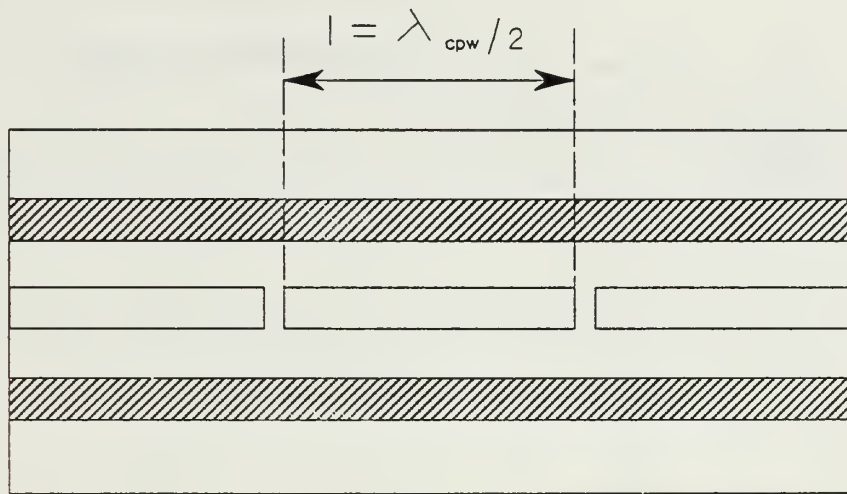
A series-connected resonator is constructed using a two port section of CBCPW connected via coaxial connectors. As shown in Figure 24 on page 34, gaps in the CBCPW center strip are separated by a half wavelength interval of coplanar line. At this length the open-ended section will act as a series-connected resonator. A gap length of a few tenths of a line width provides sufficient coupling, with minimum resonator loading.

The equivalent circuit model for a series open-ended resonator is shown in Figure 24 on page 34 as designed for use with the Touchstone CAD program. In this way, we can compare the Touchstone model for CBCPW with the results of laboratory measurement. Measurements were made to find the resonant frequency by measuring the transmission matrix element S_{21} in dB with respect to frequency. The resonant frequency occurs at minimum dB transmission loss as shown in Figure 25 on page 35.

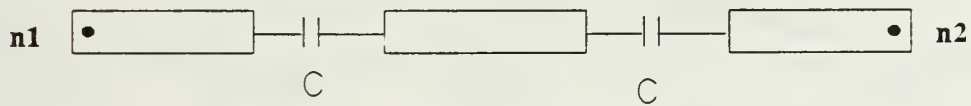
The following equations are used to find the effective dielectric constant of CBCPW by using the resonant frequency from a series open-ended resonator.

$$l = \frac{\lambda_{cpw}}{2} \quad (\text{at } f_0) \quad (43)$$

$$\begin{aligned} v_{cpw} &= f_0 \lambda_{cpw} \\ &= \frac{c}{\sqrt{\epsilon_{reff}}} \\ &= \frac{f_0 \lambda_0}{\sqrt{\epsilon_{reff}}} \end{aligned} \quad (44)$$



a : Series open-ended resonator



b : Equivalent circuit ($C = 0.005 \text{ pF}$)

Figure 24. Series open-ended resonator and equivalent circuit

therefore,

$$\begin{aligned}\epsilon_{\text{reff}} &= \left(\frac{\lambda_0}{\lambda_{\text{cpw}}} \right)^2 \\ &= \left(\frac{c}{2lf_0} \right)^2\end{aligned}\tag{45}$$

where λ_{cpw} and v_{cpw} are the wavelength and phase velocity of the waves on the CBCPW and λ_0 is the free space wavelength.

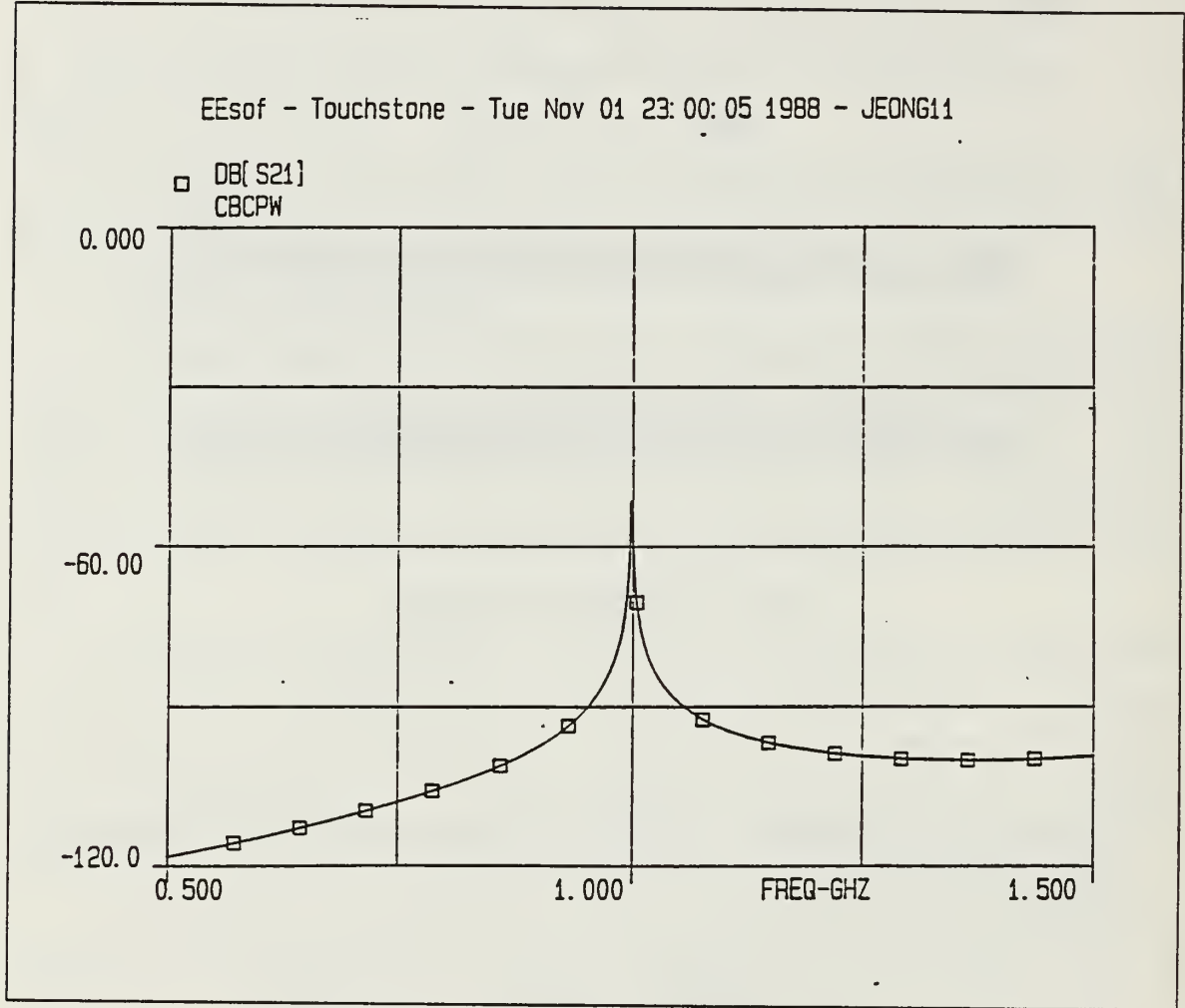


Figure 25. Plot for dB magnitude S_{21} versus frequency

The value of l used in Touchstone CAD program is 92.8 mm at a frequency of 1.0 GHz. Thus the calculated value of the effective dielectric constant at $A/H = 2.0$, $B/A = 2.0$, $C/B = 1.5$ is:

$$\begin{aligned}
 \epsilon_{\text{reff}} &= \left(\frac{c}{2lf_0} \right)^2 \\
 &= \left(\frac{3 \times 10^8}{2 \times 0.0928 \times 1.0 \times 10^9} \right)^2 \\
 &= 2.61
 \end{aligned} \tag{46}$$

2. Shunt Resonator

Two ways to calculate the resonant frequency by using a Touchstone CAD program for a CBCPW resonator are explored. One is a one-port open-ended resonator; the other is a shunt short-circuited resonator.

a. One-port Open-ended Resonator

In Figure 26 on page 36, the equivalent circuit is shown for an open-ended stub resonator for the input impedance calculation by the Touchstone CAD program. The length of the strip is a quarter wavelength. The open-ended stub input impedance is:

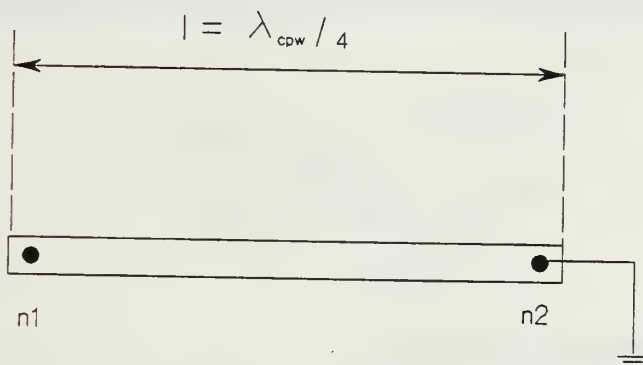


Figure 26. Equivalent circuit for calculation of angle of impedance

$$\begin{aligned} Z_{in} &= -jZ_0 \cot(\beta l) \\ &= -jZ_0 \cot\left(\frac{2\pi l}{\lambda}\right) \end{aligned} \quad (47)$$

here Z_{in} changes from a negative to a positive value at resonance, that is, the angle of Z_{in} changes from $-\frac{\pi}{2}$ radians to $+\frac{\pi}{2}$ radians. Therefore, the difference of angle of input impedance is π radians. This behavior is plotted in Figure 28 on page 39 using the Touchstone CAD program.

The equations to calculate the effective dielectric constant for the open-ended resonator are the same as for the series open-ended resonator case except that here, $l = \lambda_{cpw} / 4$.

Therefore, the final equation for calculation of the effective dielectric constant is:

$$\begin{aligned}
\varepsilon_{\text{reff}} &= \left(\frac{\lambda_0}{\lambda_{\text{cpw}}} \right)^2 \\
&= \left(\frac{\lambda_0}{4l} \right)^2 \\
&= \left(\frac{c}{4lf_0} \right)^2
\end{aligned} \tag{48}$$

where c is the velocity of light and f_0 is the resonant frequency.

The value of l used in the Touchstone CAD program is 15.45 mm to obtain a $\frac{\lambda}{4}$ resonator at a frequency of 3 GHz, based on the result of the series open-ended resonator case. Thus the calculated value of the effective dielectric constant at $A/H = 2.0$, $B/A = 2.0$, $C/B = 1.5$ is:

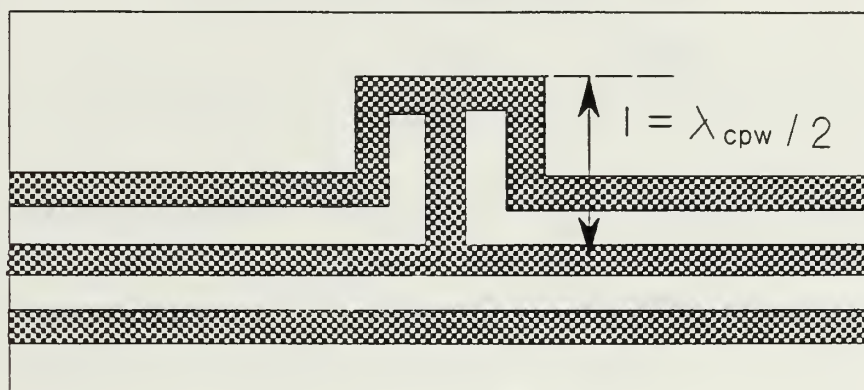
$$\begin{aligned}
\varepsilon_{\text{reff}} &= \left(\frac{c}{4lf_0} \right)^2 \\
&= \left(\frac{3 \times 10^8}{4 \times 0.01545 \times 3.0 \times 10^9} \right)^2 \\
&= 2.61
\end{aligned} \tag{49}$$

b. Shunt Short-circuited Resonator

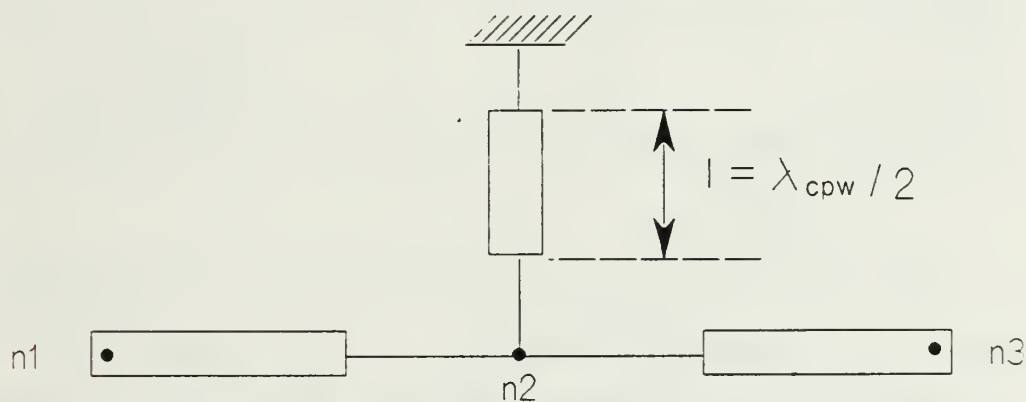
As shown in Figure 27 on page 38, a short-terminated section of CBCPW having a length of one-half coplanar-guide wavelength is connected in shunt with the through line. This is the shunt shorted resonator which models the experimental circuit shown in Figure 23 on page 31. A transmission minimum occurs at resonance. The resonant frequency of this shunt resonator can also be calculated using the Touchstone CAD program, with use of an equivalent circuit model. (See Figure 27 on page 38.) The input impedance of shunt shorted stub is:

$$\begin{aligned}
Z_{\text{in}} &= -jZ_0 \tan(\beta l) \\
&= -jZ_0 \tan\left(\frac{2\pi l}{\lambda}\right)
\end{aligned} \tag{50}$$

When l is equal to $\frac{\lambda}{2}$, the input impedance goes to zero. Therefore, a minimum value of S_{21} can be obtained from Touchstone CAD program at the resonant frequency. The resonant frequency at the minimum value of S_{21} is then used for calculation of the effective dielectric constant of the CBCPW.



a : Shunt shorted resonator



b : Equivalent circuit

Figure 27. Shunt shorted resonator and equivalent circuit

The dB magnitude output of the line section with the shunt shorted resonator is plotted in Figure 28 on page 39 and compared with the plot of the angle of input impedance of the open-ended stub. The equations to calculate the effective dielectric constant are the same in form as the series open-ended resonator, since these are both half-wavelength resonators.

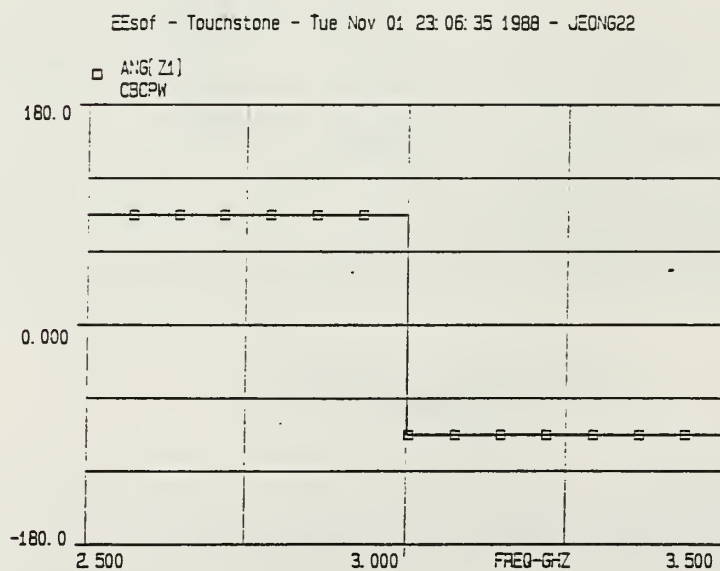
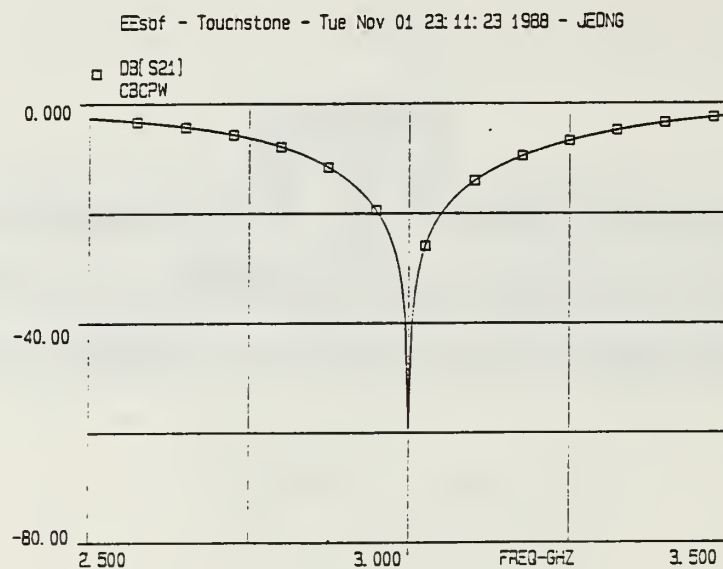


Figure 28. Plot for dB magnitude S_{21} with shunt shorted stub, and computed angle of impedance of $\frac{\lambda}{4}$ open stub at resonance

Therefore,

$$\begin{aligned}
 \epsilon_{eff} &= \left(\frac{\lambda_0}{\lambda_{cpw}} \right)^2 \\
 &= \left(\frac{\lambda_0}{2l} \right)^2 \\
 &= \left(\frac{c}{2lf_0} \right)^2
 \end{aligned} \tag{51}$$

Table 1 on page 40 contains CBCPW effective dielectric constants as calculated from the results of the two types of measurement carried out: those with the series $\frac{\lambda}{2}$ resonator and the shunt $\frac{\lambda}{2}$ resonator. The CBCPW used in these measurements had dimensions: $A = 3$ mm, $B = 6$ mm, $C = 9$ mm.

Table 1. COMPARISON OF THE EFFECTIVE DIELECTRIC CONSTANT

Item	Effective dielectric constant (f_0)	
	Touchstone	Measured
Series open-ended stub ($l = 92.8$ mm)	2.61 (1 GHz)	2.61 (1 GHz)
Shunt shorted stub ($l = 30.9$ mm)	2.61 (3 GHz)	2.68 (2.96 GHz)

B. LEAKAGE WAVE MEASUREMENTS ON COPLANAR LINE AND MICROSTRIP

Conductor backed coplanar waveguide (CBCPW) transmission line is compared to microstrip in terms of relative extent of the ambient fields around the lines. An angle section is used so that the fields both around a corner and straight sections may be observed. The angle section is expected to be a worst case due to the greater magnetic-energy storage in the neighborhood of the corner.

1. Measurement

The steps are:

1. Choose the dimensions of CBCPW for 50Ω impedance by using the Rowe and Lao method (substrate height is $H = 1.5$ mm, dielectric constant $\epsilon_r = 3.52$).
2. Design an angle stub (See Figure 29 on page 41) to measure the fields near the conductor at the angle point.
3. Make a small loop antenna to detect the leakage wave (diameter = 10 mm) (see Figure 30 on page 41).

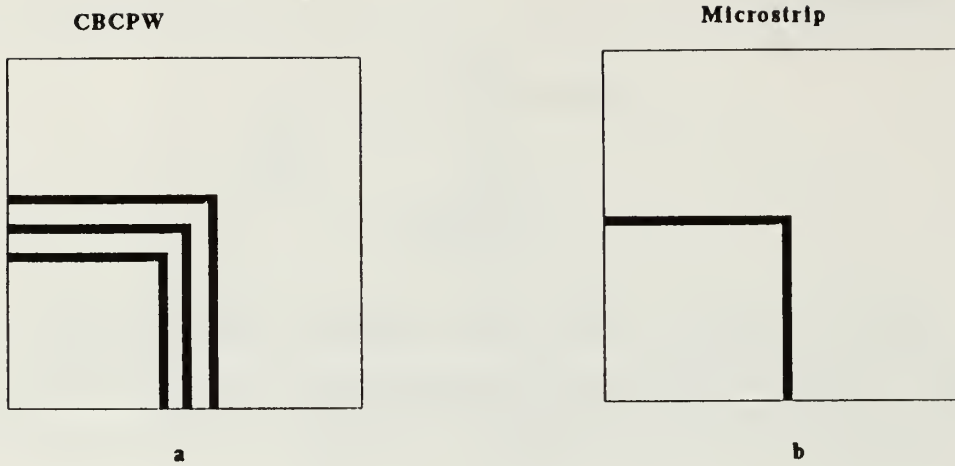


Figure 29. Line angle for conductor ambient field measurement

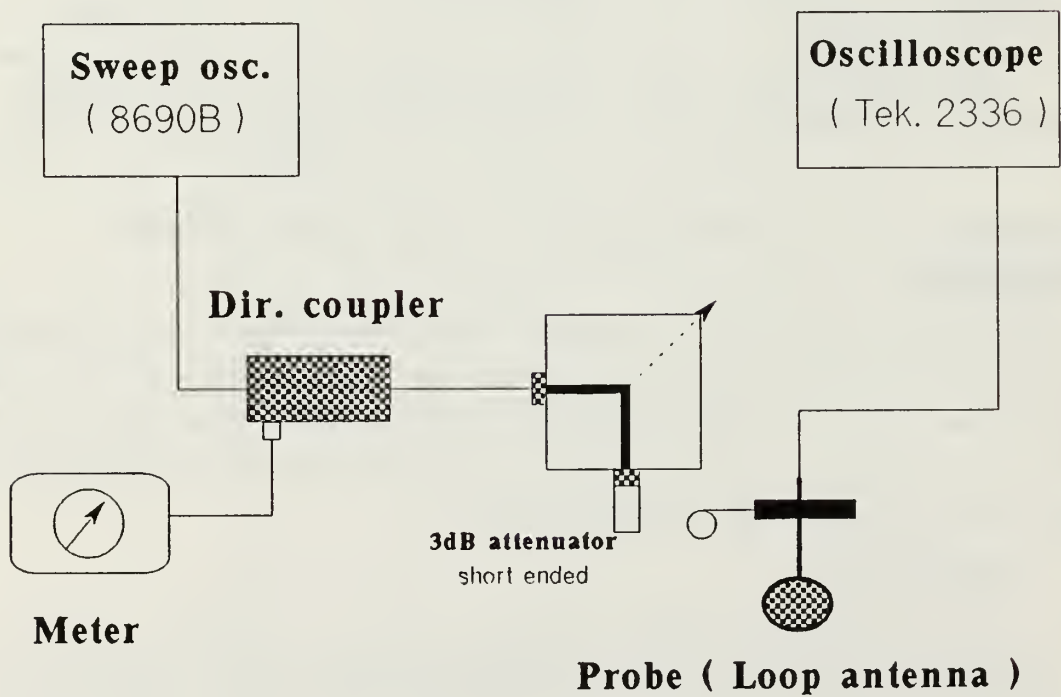


Figure 30. Block diagram for conductor ambient field measurement

4. Move this probe (loop antenna) in a straight line from the middle point of the center conductor of the angle portion to outside of the line.
5. Read the oscilloscope output and plot the results to compare the outputs of microstrip and CBCPW.

Although as is true in all such field-probing measurements, the electromagnetic fields are perturbed by the presence of the probe, and no field details smaller than the size of the probe can be observed, a useful comparison of the two cases (coplanar line and microstrip) observed can be obtained.

2. Results

Figure 31 on page 43 shows the probe measurement plotted against the distance for microstrip and CBCPW on 1.5 mm thick substrate with a relative permittivity of 3.52 at 3 GHz. A thin copper conductor, which is designed by the photolithographical method, is chosen.

For a given substrate thickness and dielectric constant, CBCPW has a lower ambient field strength than microstrip. The spurious coupling between adjacent coplanar lines is therefore expected to be significantly lower than with microstrip.

COMPARISON OF CONDUCTOR AMBIENT FIELD

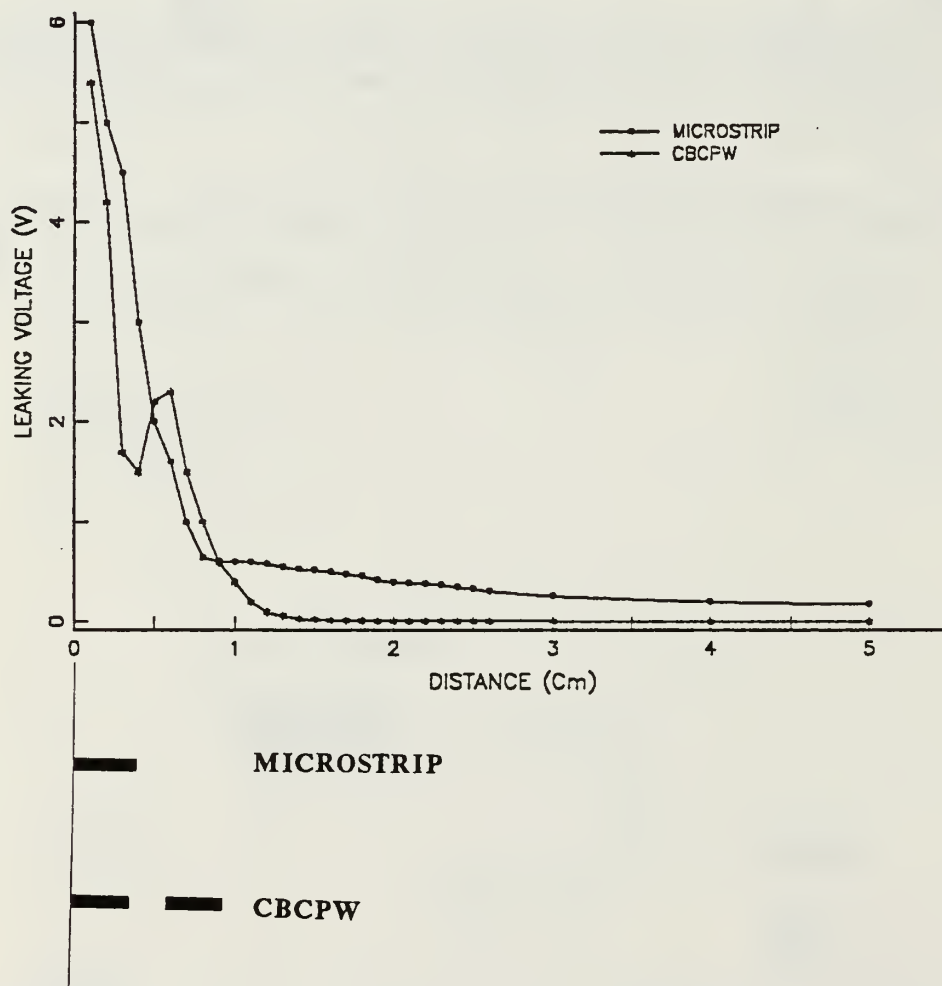


Figure 31. Conductor ambient field distribution

V. SUMMARY AND CONCLUSION

In the foregoing investigation, conductor backed coplanar lines on finite-height substrate have been investigated. (In this present work, substrate height $H = 1.5$ mm, dielectric constant $\epsilon_r = 3.52$.) This is a typical form for use in microwave integrated circuitry.

The research has included:

1. Calculation of the effective dielectric constant and characteristic impedance of conductor backed coplanar waveguide.
2. Construction of coplanar lines and a transition from CBCPW to a coaxial connector.
3. Measurements of CBCPW parameters (phase velocity and effective dielectric constant) on practical line sections.

Two computational methods, the boundary point matching method and the variational method, were used to calculate the effective dielectric constant and impedance for various line dimensions. The impedances and effective dielectric constant obtained from the variational method are compared with values obtained from the boundary point matching method as computed for similar line parameters. The results of both methods are in good agreement. For impedance (Z_0), Figure 13 on page 20 through Figure 16 on page 23 show that less than 6 % difference was observed for most cases, and less than 5 % difference in the dielectric constant is shown in Figure 17 on page 24 through Figure 20 on page 27.

For a large aspect ratio A/H , impedance shows little change versus the ratio B/A , since both slot coupling effects and the effects of fringing fields are relatively small with large A/H ratio. A wider gap causes a larger impedance, and the microstrip characteristic behavior will be approached when the gap goes to infinity or zero. Therefore, by adjusting both slot widths and center strip width, independent control of the characteristic impedance can be obtained.

Figure 32 on page 46 and Figure 33 on page 47 show that the impedance and the effective dielectric constant of CBCPW are changed appreciably with increasing dielectric constant of the substrate. The choice of proper dielectric constant of substrate is therefore very important. A method for calculating this dielectric constant of the substrate material is detailed in Chapter III (A).

As was mentioned in Chapter I (Introduction), CBCPW has a smaller extent of ambient fields than does microstrip. The spurious coupling between coplanar lines and adjacent circuitry is thus lower than with microstrip. This behavior is demonstrated in Chapter IV, through leakage field measurements on coplanar line and microstrip.

In Chapter III, two methods for fabrication of CBCPW are considered, and we infer that the photolithographical method is better than the adhesive foil method due to its inherently greater accuracy. Also the three special requirements of CBCPW transition to coaxial line are described.

These three requirements are:

1. Top and bottom ground plane connector.
2. Connection lead length as short as possible.
3. Smooth mechanical transition between physical components to avoid parasitics.

Phase velocity and effective dielectric constant of CBCPW can be calculated by using two kinds of resonator: series open-ended and shunt shorted, as described in Chapter IV. This consideration gives the following points. The series resonator must be lightly coupled in order to avoid pulling of the resonant frequency. In the present work the parasitic capacitance to ground of the open ends was unaccounted for, but these values, as inferred from the corresponding microstrip case, are typically small.

The availability of design data for conductor backed coplanar line will facilitate the use of this transmission format in microwave integrated circuit design. It is anticipated that the results of this study will promote a better understanding of coplanar waveguide, and promote its use in practical microwave circuits.

ROWE AND LAO METHOD IMPEDANCE

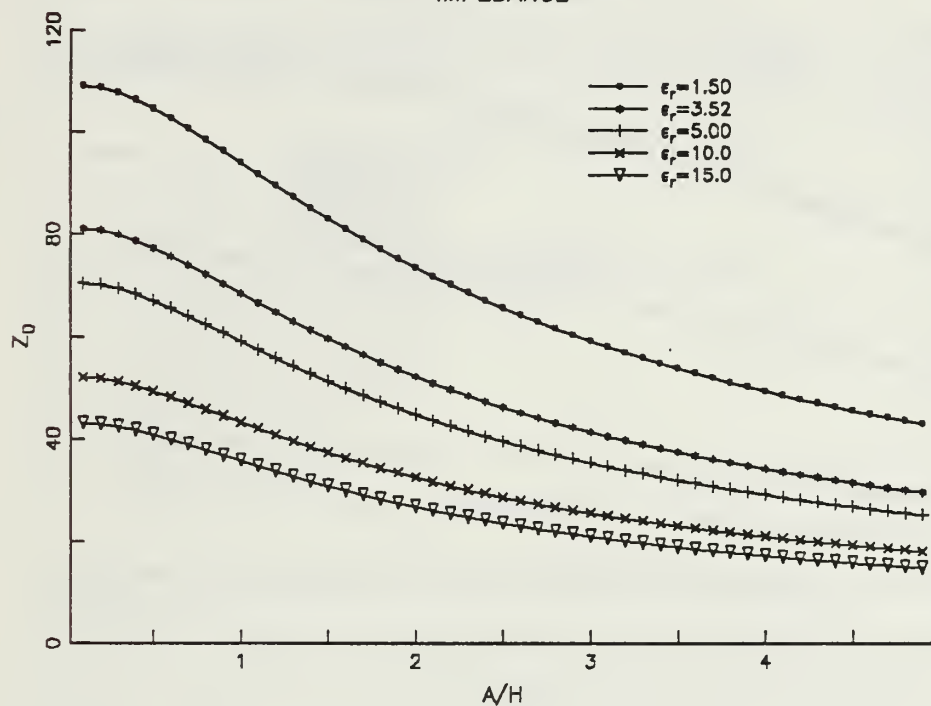


Figure 32. Characteristic impedance versus strip width with dielectric constant as a parameter: ($B/A = 2.0$, $C/B = 2.0$, $H = 1.5$ mm)

ROWE AND LAO METHOD
EFFECTIVE DIELECTRIC CONSTANT

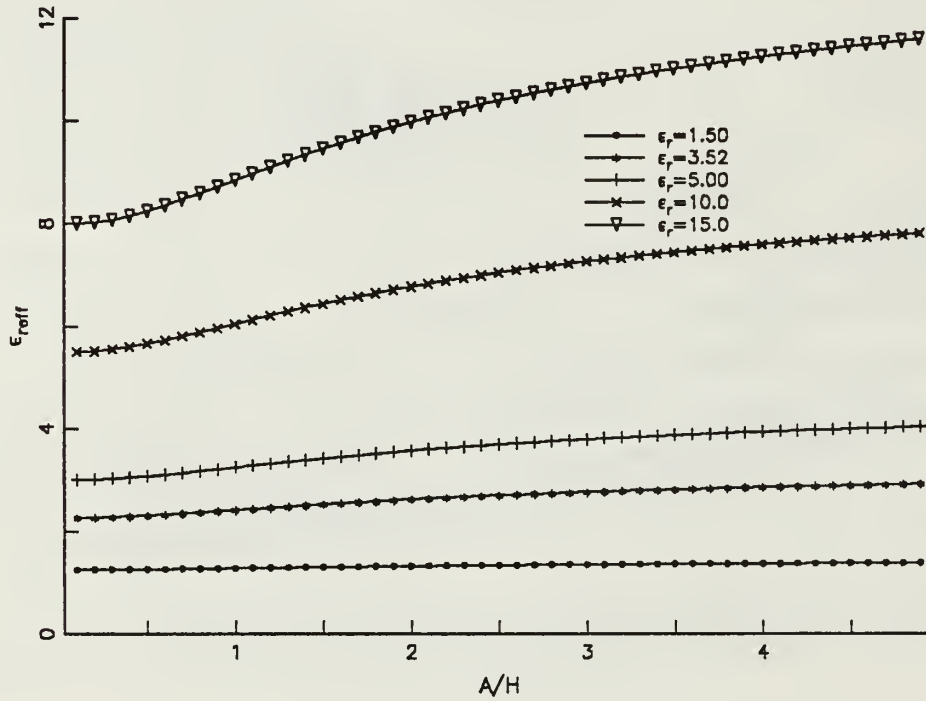


Figure 33. Effective dielectric constant versus strip width with substrate dielectric constant as a parameter: ($B/A = 2.0$, $C/B = 2.0$, $H = 1.5$ mm)

APPENDIX A. FORTRAN PROGRAM TO CALCULATE THE IMPEDANCE AND EFFECTIVE DIELECTRIC CONSTANT OF CBCPW USING BOUNDARY POINT MATCHING METHOD

C\$NOEXT

```

C      *****  PURPOSE  *****
C
C      TO CALCULATE THE IMPEDANCE AND EFFECTIVE DIELECTRIC CONSTANT
C      OF CBCPW BY USING BOUNDARY POINT MATCHING METHOD

```

```

C      *****  VARIABLE DEFINITIONS  *****
C
C      H      = SUBSTRATE HEIGHT
C      ER      = DIELECTRIC CONSTANT OF SUBSTATE
C      ERE     = EFFECTIVE DIELECTRIC CONSTANT OF CBCPW
C      C1      = CAPACITANCE FOR ER = 3.52
C      C0      = CAPACITANCE FOR ER = 1.0
C      Z0      = IMPEDANCE OF CBCPW
C      V      = VELOCITYOF LIGHT
C      AA      = RATIO OF A/H
C      BB      = RATIO OF B/A
C      CC      = RATIO OF C/B

```

```

REAL*8 H,ER,K,M,A,B,C,G,L,C0,C1,Z0,ERE,V,AA,BB,CC
V=3. D+08
OPEN(UNIT=7,FILE='RLM DATA')

```

```

10  PRINT*, 'HOW MANY POINTS FOR CALCULATING THE IMPEDENCE (Z0)?'
    READ(*,*)N
    PRINT*, 'THICKNESS OF SUBSTRATE (H(M))?'
    READ(*,*)H
    PRINT*, 'ER=?'
    READ(*,*)ER
    PRINT*, 'A/H=?'
    READ(*,*)AA
    PRINT*, 'B/A=?'
    READ(*,*)BB
    PRINT*, 'C/B=?'
    READ(*,*)CC
    A=AA*H/2. D00
    B=BB*A
    C=CC*B
    L=2. D00*C

    CALL LAO(N,H,1. D00,A,B,C,L,C0)

    CALL LAO(N,H,ER,A,B,C,L,C1)

```



```

ERE=C1/C0
Z0=(1.D00/V)/SQRT(C1*C0)

WRITE(7,33)AA,BB,CC,Z0,ERE
33  FORMAT(3(1X,D8.4),2(1X,D9.5))

PRINT*, 'IF YOU WANT TO RUN AGAIN, ENTER (22)'
READ(*,*)MM
IF(MM.EQ.22)GOTO 10
STOP
END

C  *****
C  SUBROUTINE LAO(N,H,ER,A,B,C1,L,C)
C  *****

REAL*8 K(N),X(N),M(N,N),T(N,N+1),D(N),AA(N)
#      ,H,ER,A,B,G,L,Z0,ERE,PHI,E0,C0,C,V,C1

PHI=4.D00*DATAN(1.D00)
E0=1D-09/(36*PHI)
C=0

DO 100 I=1,N
  K(I)=(2*I-1)*PHI/(2*L)
  DO 200 J=1,N
    X(J)=J*L/(N+1)
    IF((X(J).GT.A.AND.X(J).LT.B).OR.X(J).GT.C1)THEN
      M(J,I)=K(I)*COS(K(I)*X(J))*(1+ER*1/TANH(K(I)*H))
    ELSEIF((X(J).GE.B.AND.X(J).LE.C1).OR.X(J).LE.A)THEN
      M(J,I)=COS(K(I)*X(J))
    ELSE
      PRINT*, 'SORRY, WRONG APPLY. CHECK INPUT DATA AGAIN!'
    ENDIF
    T(J,I)=M(J,I)
    IF(X(J).GT.A)D(J)=0
    IF(X(J).LE.A)D(J)=1
200    CONTINUE
    T(I,N+1)=D(I)
100  CONTINUE

CALL GAUSS(T,N,N+1,AA)

DO 300 I=1,N
  C=AA(I)*SIN(K(I)*(A+B)/2)*(1+ER*1/TANH(K(I)*H))+C
300  CONTINUE
  C=-2.D00*E0*C
RETURN
END

```

```

C      *****
C      SUBROUTINE GAUSS(A,N,L,X)
C      *****

C      ---- SOLUTION BY GAUSSIAN ELIMINATION ----

      REAL*8 A(N,N+1),X(N)
      NN=N-1

      DO 99 K=1,NN
        CALL FIND(A,N,N+1,K,J)
        CALL CHANGE(A,N,N+1,K,J)
        KK=K+1

        DO 88 I=KK,N
          CALL ROWMUL(A,N,N+1,K,I,-A(I,K)/A(K,K))
88      CONTINUE
99      CONTINUE

      CALL BKSUB(A,N,N+1,X)

      RETURN
      END

C      *****
C      SUBROUTINE FIND(A,N,L,K,J)
C      *****

C-- FIND THE LARGE VALUE( TO AVOID THE FLOATING POINT DIVIDED ZERO)----

      REAL*8 A(N,N+1)
      J=K
      KK=K+1

      DO 100 I=KK,N
        IF (ABS(A(J,K)).LT.ABS(A(I,K))) J=I
100    CONTINUE

      RETURN
      END

C      *****
C      SUBROUTINE CHANGE(A,N,L,K,J)
C      *****

C-- CHANGE THE ROW ( TO AVOID THE FLOATING POINT DIVIDED ZERO )-----

```

```

REAL*8 A(N,N+1)
IF (J.EQ.K)RETURN

DO 100 I=1,L
    T=A(K,I)
    A(K,I)=A(J,I)
    A(J,I)=T
100 CONTINUE

RETURN
END

C *****
C SUBROUTINE ROWMUL(A,N,L,K,J,D)
C *****

C ---- ROW MULTIPLICATION ----

REAL*8 A(N,N+1),D

DO 100 I=1,L
    A(J,I)=A(J,I)+D*A(K,I)
100 CONTINUE

RETURN
END

C *****
C SUBROUTINE BKSUB(A,N,L,X)
C *****

C ---- FIND THE RESULT OF X(K) ----
C
REAL*8 A(N,N+1),X(N)
X(N)=A(N,N+1)/A(N,N)
NN=N-1

DO 100 J=1,NN
    K=N-J
C ---- CALCULATING SUM FOR X(K) ----
    SUM=0.0
    NNN=N-K

    DO 200 JJ=1,NNN
        M=K+JJ
        SUM=SUM+A(K,M)*X(M)
200 CONTINUE

C ---- SOLVING FOR X(K) ----

```

```
      X(K)=(A(K,N+1)-SUM)/A(K,K)
100  CONTINUE

      RETURN
      END
```

APPENDIX B. FORTRAN PROGRAM TO CALCULATE THE IMPEDANCE AND EFFECTIVE DIELECTRIC CONSTANT OF CBCPW USING VARIATIONAL METHOD

C\$NOEXT

```
C      *****  PURPOSE  *****
C      TO CALCULATE THE IMPEDANCE AND EFFECTIVE DIELECTRIC CONSTANT
C      OF CBCPW BY USING VARIATONAL METHOD.
```

```
C      *****  VARIABLE DEFINITIONS  *****
C      H      = SUBSTRATE HEIGHT
C      ER      = DIELECTRIC CONSTANT OF SUBSTATE
C      ERE     = EFFECTIVE DIELECTRIC CONSTANT OF CBCPW
C      CD      = CAPACITANCE FOR ER = 3.52
C      CO      = CAPACITANCE FOR ER = 1.0
C      ZO      = IMPEDANCE OF CBCPW
```

```
REAL Q0,Q,A,B,C,ER,ERE,PI,H,M1,CD,CO,ZO
EXTERNAL F
COMMON H,A,B,C,Q0,Q,PI,M1,ER
OPEN(UNIT=2,FILE='VM DATA')
```

```
DATA AERR,RERR,A1,B1/1.E-06,0,0.1E-30,3.4E03/
```

```
PI=4.*ATAN(1.)
Q0=1.0
M1=4.0E-02
H=0.0015
ER=3.52
```

```
A=2.1*H
B=1.0*A
C=2.0*B
```

```
Q=Q0*A/2.+M1*(B-C)
```

```
S1=PI*8.84*1.E-12*Q**2
```

```
S2=DCADRE(F,A1,B1,AERR,RERR,ERROR,IER)
```

```
ER=1.0
```

```
S3=DCADRE(F,A1,B1,AERR,RERR,ERROR,IER)
```

```
CD=S1/S2
CO=S1/S3
```

```

ERE=CD/CO
ZO=1. /(3.*1.E08*SQRT(CD*CO))

11  WRITE(2,11)A/H,B/A,C/B,ZO,ERE
    FORMAT(1X,5(F14.8))
    STOP
    END

C   *****
C   REAL FUNCTION F(BB)
C   *****

REAL Y1,Y2,A,B,C,H,QO,ER,BB,M1
COMMON H,A,B,C,QO,Q,PI,M1,ER

Y1=(Q*(4.*SIN(BB*A/(2.)))/(BB*A)-(4.*SIN(BB*A/(4.)))/
#(BB*A))*2)+2*M1/BB*(SIN(BB*B/2.)-SIN(BB*C/2.))*2

Y2=BB*(1+ER/TANH(BB*H))

F=Y1/Y2

RETURN
END

```

LIST OF REFERENCES

1. Leuzzi, G, *Mode Propagation in Laterally Bounded Conductor Backed Coplanar Devices*, IEEE International Microwave Symposium (1983), pp. 393-395.
2. Riazat, M, *Coplanar Waveguide Used in 2-18 GHz Distributed Amplifier*, IEEE International Microwave Symposium (1986) pp. 337-338.
3. Jackson, R. W, *Considerations in the Use of Coplanar Waveguide in Integrated Circuits*, IEEE Transaction Microwave Theory Technology, Vol. MTT-34, pp. 1450-1456 (1986).
4. Wen, C. P, *Coplanar Waveguide, A Surface Strip Transmission Line*, IEEE Transaction Microwave Theory Technology, Vol. MTT-17, pp. 1087-1090 (1969).
5. Schulz, U and Pregla, R, *The Method of Lines for Planar Waveguide, Demonstrated for the Coplanar Line*, Proceedings 10th European Microwave Conference (1980), pp. 331-335.
6. Shih, Y and Itoh, T, *Analysis of Conductor Backed Coplanar Waveguide*, Electronics Letters, Vol. 19, pp. 734 (1983).
7. Rowe, D. A and Lao, B. Y, *Numerical Analysis of Shielded Coplanar Waveguide*, IEEE Transaction Microwave Theory Technology, Vol. MTT-31, pp. 911-915 (1983).
8. Yamashita, E and Mittra, R, *Variational Method for the Analysis of Microstrip Lines*, IEEE Transaction Microwave Theory Technology, Vol. MTT-16, pp. 251-256 (1968).
9. Yamashita, E, *Variational Method for the Analysis of Microstrip Like Transmission Lines*, IEEE Transaction Microwave Theory Technology, Vol. MTT-16, pp. 529-535 (1968).

INITIAL DISTRIBUTION LIST

	No. Copies
1. Defense Technical Information Center Cameron Station Alexandria, VA 22304-6145	2
2. Library, Code 0142 Naval Postgraduate School Monterey, CA 93943-5002	2
3. Chairman, Code 62 Department of Electrical and Computer Engineering Naval Postgraduate School Monterey, CA 93943-5000	1
4. Curricular Officer, Code 32 Department of Electrical and Computer Engineering Naval Postgraduate School Monterey, CA 93943-5000	1
5. David Rubin, Code 753 Microwave Circuit Laboratory Naval Ocean Systems Center San Diego, CA 92152	1
6. Robert J. Dinger Research Department Naval Weapons Center China Lake, CA 93555-6001	1
7. Prof. H.A. Atwater, Code 62An Department of Electrical and Computer Engineering Naval Postgraduate School Monterey, CA 93943-5000	1
8. Prof. R. Janaswamy, Code 62Js Department of Electrical and Computer Engineering Naval Postgraduate School Monterey, CA 93943-5000	1
9. Air Force Central Library Sindaebang Dong, Gwuanak Gu, Seoul, Republic of Korea	2
10. Library of Air Force Academy Cheongwon Gun, Chung Cheong Buk Do, Republic of Korea	2

- | | | |
|-----|---|---|
| 11. | Jeong, Jae Soon
307dong 102ho Sanggye Joogong APT.,
Sanggye Dong, Nowon Gu, Seoul,
Republic of Korea | 2 |
| 12. | Choi, Man Soo
SMC 1142 NPS
Monterey, CA 93943 | 1 |

Thesis

J4748 Jeong

c.1 An evaluation of coplanar line for application in microwave integrated circuitry.

Thesis

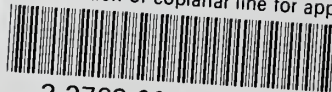
J4748 Jeong

c.1 An evaluation of coplanar line for application in microwave integrated circuitry.



thesJ4748

An evaluation of coplanar line for appli



3 2768 000 81621 9

DUDLEY KNOX LIBRARY